Sensitivity Study of Knee Ligament Properties in a Computer Simulation of a Total Knee Arthroplasty

Undergraduate Honors Research Thesis

Presented in Partial Fulfillment of the Requirements for
Graduation with Distinction in the
Department of Mechanical Engineering at
The Ohio State University

Michelle Cullen

January 30, 2014

Advisor: Robert A. Siston, Ph.D.

Abstract

Total knee arthroplasty (TKA) is a common, end-of-stage surgical treatment for osteoarthritis. It is widely believed that surgical technique has a large influence on patient function after TKA. Computer simulation of TKA is a valuable tool for establishing an objective connection between surgical technique and postoperative function. However, there is little consensus on how to accurately model ligaments surrounding the knee and a lack of understanding of how modeling choices influence simulated TKA kinematics. The purpose of this study was to systematically investigate the sensitivity of variations in ligament modeling parameters on simulated TKA kinematics. 850 simulations with the knee in full extension were run with the following modeling variations of the medial and lateral collateral ligaments (MCL and LCL): increasing and decreasing slack length by 2.5 and 5%, increasing and decreasing stiffness by 25, 50, and 75%, varying attachment sites of the ligaments by translating 1 cm in the two anatomical directions and crossing ligament fibers, and increasing the number of fibers from two to four. An applied force versus varus/valgus angle curve was calculated from the output of each simulation. The specimen-specific simulation of TKA motion showed clear differences in the varus/valgus behavior of the knee with varying ligament modeling choices. These results suggest that ligament slack length has the greatest impact on varus/valgus laxity. Increasing the number fibers of the MCL affected the varus/valgus laxity and indicated sensitivity to the anterior/posterior location of the additional fibers. Understanding the sensitivity of ligament modeling choices informs the creation of computer simulations of TKA motions that can provide reliable insight of how surgical technique influences knee function after TKA.

Acknowledgements

The project could not have been completed without the contributions of several individuals. I owe Dr. Robert Siston the greatest thanks for his continuous support, patience, and encouragement during my time in his lab. Thank you for having confidence in my ability to improve and constantly reminding me I was capable of completing this research. I have learned considerably more about writing, presenting, thinking, and trusting my knowledge and abilities by being involved in research than I ever would have by just completing my undergraduate degree.

I owe a HUGE thank you to Joe Ewing for his guidance and encouragement over the last year and a half. Joe was always a patient teacher and spent countless hours explaining (and re-explaining) components of this project. Without all of his help to understand concepts and write and debug code, this research would not have been possible. Thank you for letting me actively participate in the cadaver study and tag along to the operating room.

I would also like thank Dr. Ajit Chaudhari for being a part of my committee; I very much appreciate your time and support of my research. I also owe a thank you to Dr. Stephen Piazza for suggesting alternative methods and reviewing results over the course of the project.

I would very much like to thank my NMBL lab mates, especially Dr. Erin Hutter for providing several hints and pieces of code, narrating procedures in the operating room, and patiently explaining concepts throughout my project. As well, I owe a huge thank you to Dr. Julie Thompson and Becky Lathrop for being fantastic role models and welcoming lab leaders. Becky and Julie always took time to assist with printer issues, help calm nerves, enter administrative passwords, chat over lunch, and support me in other simple yet meaningful

ways. I have always felt like a welcomed member of this lab because of their gestures. Thank you to the rest of my NMBL lab mates for listening to several practice presentations and providing opinions and constructive criticism.

I owe a very special thank you to Katie Woodling for sticking by my side over the last three years. I can confidently say I would have not been successful in my college career without her patience and help through classes and life beyond the lab. She deserves thanks for not only proofreading chapters and posters and listening to presentations, but for suppressing panic and pushing me through tough spots when I was extremely ready to give up. I have no regrets about dragging her into Dr. Siston's office to discuss undergraduate research because the experience would not have been nearly as fun, competitive, or worthwhile without her.

Finally, I would like to thank my family and friends who have encouraged and stood behind me, not only during this project, but over my five undergraduate years. The dinner dates, phone calls, care packages, coffee breaks, and constant love from so many people are the reasons this research (and college experience) have been so rewarding.

Table of Contents

List of Figures

List of Tables

Chapter 1: Introduction

Osteoarthritis (OA) is a common, degenerative joint disease that causes painful movement, limited range of joint motion, and severe joint tenderness. As people age, the cartilage in joints throughout the body deteriorates, and results in bone on bone contact. Osteoarthritis affected approximately 45.5 million adults in 2003, and is projected to affect 67 million adults in 2030 [1] . In 2003, approximately 16.9 million adults reported that their arthritis was the cause of activity limitations. Roughly 17.6 million adults are projected to experience activity limitations due to arthritis in 2030 [1] .

Specially, osteoarthritis in the knee joint affects 10 million American adults [2]. A total knee arthroplasty (TKA) is a cost effective surgical repair of the knee joint and a common end-stage treatment for osteoarthritis of the knee. Roughly 600,000 TKAs are performed a year [3, 4]. By 2030, demand for TKAs is predicted to reach at least 3.48 million procedures in the United States alone [3].

A TKA is generally considered successful if the patient is relieved of joint pain and there is improvement over the preoperative condition [5]. However, postoperative functionality after TKA can be highly variable, affecting a patient's ability to perform important everyday functions such as walking, climbing stairs, kneeling, and squatting [6]. In one study, 50% of TKA patients were unable to climb a 20-cm step [7]. In a self-assessment survey of 176 TKA patients one year after surgery, approximately 75% reported trouble kneeling and squatting [6]. Even when TKA patients are able to ascend stairs, they do so at a significantly slower speed than age-matched people with healthy knees [8].

TKA outcomes are influenced by preoperative joint condition, surgical technique, component alignment, and postoperative rehabilitation [9, 10]. Surgical technique has a strong influence on postoperative function and includes two main tasks: prosthetic component placement and soft tissue balancing [9-11]. Soft tissue balancing is defined as the management of the ligaments and tissues surrounding the knee. After TKA, typically only the medial collateral ligament (MCL) and lateral collateral ligament (LCL) remain intact and surgeons attempt to stabilize the joint by ensuring these two ligaments have an equal amount of force. While some published practices for ligament balance exist [11, 12], none of these practices are universally accepted due to a lack of objective understanding of the cause-effect relationship between surgical technique and the patient's postoperative functionality [13]. Surgeons typically manually manipulate the knee joint and visually determine if the knee is 'stable'. Although skilled surgeons determine what a stable joint 'feels' like, this subjective feel is not confirmed by an objective measurement of the forces in the collateral ligaments to define joint stability [13].

The use of dynamic computer simulations of a TKA knee can be helpful in understanding the cause-effect relationship between surgical technique and postoperative function [14]. A computer simulation of a TKA knee performing fundamental tasks (e.g., walking, climbing stairs, squatting, etc.) can be used to study how component alignment and ligament balancing affect surgical outcome [15, 16].

Several studies have investigated how component placement and design influence the forces and motion in a simulated TKA knee. Femoral component alignment was found to have the most significant effect on ligament forces while tibial component alignment had the most

effect on knee varus-valgus angle [17, 18]. Implant design differences, such as increased posterior tilt of the tibial component (in a PCL-substituting TKA) reduced the range of flexion [19]. These simulation studies on component alignment and design have illustrated how component placement affects ligament forces and knee motion. However, very few studies have investigated how the ligaments themselves influence simulated TKA motion and forces due to lack of understanding of how to model the ligaments surrounding the knee.

There are various limitations to modeling ligaments in a TKA simulation. Ligament property values (e.g., stiffness, slack length) used in most simulations trace back to just a few studies on healthy (non-osteoarthritic) cadaveric specimens [20-30]. However, these ligament properties from healthy cadavers may not be applicable to knees with osteoarthritis.

Additionally, ligament modeling choices vary between different simulations. Current simulations vary in modeling strategies of the number of bands used to represent each ligament, the location of discrete attachment site of the ligament to the bone, and the wrapping surfaces between the ligament bands and boney landmarks [15, 16, 31-33]. However, these modeling choices are arbitrarily chosen, and no one modeling choice is considered 'correct'.

It is not understood how ligament modeling choices and ligament properties in a computer simulation of a TKA impact the motion and force in the knee joint. This research systematically alters four ligament modeling choices to understand the simulation's sensitivity on the following outputs: varus-valgus angle, force in the MCL, LCL, and posterior capsule, and contact force between the femoral and tibial components.

1.1 Focus of Thesis

This research uses a forward-dynamic simulation of varus-valgus motion in a TKA knee at different degrees of knee flexion to systematically investigate the sensitivity of four modeling choices that are used to model the LCL, MCL, and posterior capsule. The goal of this project was to determine which of these modeling choices most impact the varus-valgus angle in a simulated TKA, individually and in combinations.

1.2 Significance of Research

While a TKA is considered successful at reliving pain caused by osteoarthritis of the knee, not all surgeries leave patients satisfied with their ability to perform everyday tasks. Therefore, it is of interest to researchers to investigate the cause and effect connection between surgical technique and postoperative function; computer simulations provide a noninvasive method to understand how changes in component placement and ligament balancing techniques impact the patient's function after surgery. However, current simulations are built with varying modeling strategies, and none are considered 'correct'. This research investigates the sensitivity of ligament modeling choices in a simulation of a TKA. These results can be combined with studies on prosthetic component placement to produce a more realistic simulation of TKA. A computer simulation can provide a more objective understanding of the connection between surgical technique and postoperative function. By understanding how ligament modeling choices impact knee motion, researchers can hopefully build patient-specific simulations to predict postoperative function based on surgical technique.

Chapter 2: Literature Review

While computer simulations of the knee joint are commonly used, there is great variability in how they are constructed. Various modeling choices that are made in creating simulations are adapted from cadaver studies or appear to be arbitrarily chosen. These modeling decisions include, but are not limited to: inclusion/exclusion of soft tissues and muscles, soft tissue and muscle properties, bone geometry, ligament wrapping and attachment sites, number of elements used to represent collateral ligaments and posterior capsule, joint contact, type of simulation (i.e., quasi-static, dynamic, finite element, lumped parameter), and simulation inputs and outputs. In this chapter, a literature review is summarized to illustrate the variability in modeling choices with regard to soft tissue properties (stiffness and slack length), attachment site, and the number of bands in previous models and simulations. This chapter highlights the necessity of a parametric study to determine which modeling choices significantly affect the outputs (i.e. kinematics and forces) of simulations.

The material properties of the cruciate and collateral ligaments used to create computer simulations come from cadaver studies. These cadaver studies have investigated the stiffness [20, 23, 27, 29, 30], strain [20, 22, 26, 27, 29, 30], laxity [23-25], length [21], rupture force [20, 26, 27, 29], recruitment [21, 24, 25, 28, 34], and attachment sites [22, 28] of the ligaments surrounding the knee. However, there are limitations to using these findings in the construction of models and simulations.

2.1 Cadaver data

One limitation to using information from these previous cadaver studies is that all of the specimens used were natural/native knees, and the majority of the knees had no known pathologies. [20-30, 34]. Many models and simulations are used to study the natural knee [31,

32, 35-47] and the properties found in these cadaveric studies may be representative of that specific population. Other models and simulations are utilized to investigate total knee arthroplasty [10, 15, 16, 45, 48-55]. Individuals who undergo TKA have an advanced stage of OA. When OA is present in the knee it is known that the properties of ligaments are different than those in healthy knees [56]. Therefore, models and simulations using properties from a small sample of healthy, typically older cadaver knees may not be applicable to all living subjects.

Another limitation of referencing previous cadaver studies as a basis for simulations is that not all cadaver studies have large sample sizes. Arbitrary sample sizes of cadavers of different age ranges may not be representative of large portions of the population (Table 1).

Table 1: Cadaver specimen information reported in literature. The number of cadavers, mean age, age range, and sex of the cadaver samples vary significantly across studies.

Study	**# of cadavers**	**Range** [yrs]	**Mean** [yrs]	**Sex** [M/F]
Brantigan [21]	100	-	-	-
Edwards [22]	4	-	-	-
Trent [20]	10	29-55	-	-
Markolf [23]	35	53-78	64	17 M, 18 F
Hsieh [24]	8	39-71	-	-
Grood [25]	16	18-55	37	9 M, 2 F
Butler [30]	3	21-30	27	1 M, 2 F
Blankevoort and Huiskes [28]	4	43-74	61	1 M, 3 F
Quapp [26]	10	44-80	62	9 M, 1 F
Robinson [27]	8	-	77	-
Griffith [34]	24	45-87	70	-
Wijdicks [29]	20	27-68	54	-

2.2 Ligament modeling

There are also inconsistencies as to how ligament properties are defined in modeling and simulation studies. These properties (stiffness and reference strain) are either adaptations

of ligament properties from cadaver studies or taken from previous model and simulation studies [16, 32, 38-43, 45-49, 57, 58] (Figures 1 and 2). However, these properties are not defined in the same way. Stiffness is traditionally defined as a force per unit length. However, many simulations are constructed using different definitions of stiffness (Table 4). These varying definitions make it difficult to compare the values used across different studies. Additionally, the mathematical explanations of these 'adaptations' are often not reported in the literature. The length characterization of ligaments also varies across models and simulations (Table 5). Some studies choose to define the slack length (length of the ligament when it first sees tension) [15, 43], reference length (length of the ligament in full extension) [59], distance between two attachment sites [51], or reference strain (displacement of ligament from length in full extension to various degrees of flexion) [16, 26, 31, 33, 36, 38, 42, 44, 46, 48]. This variability in how ligament properties are defined makes it difficult to establish comparisons between studies.

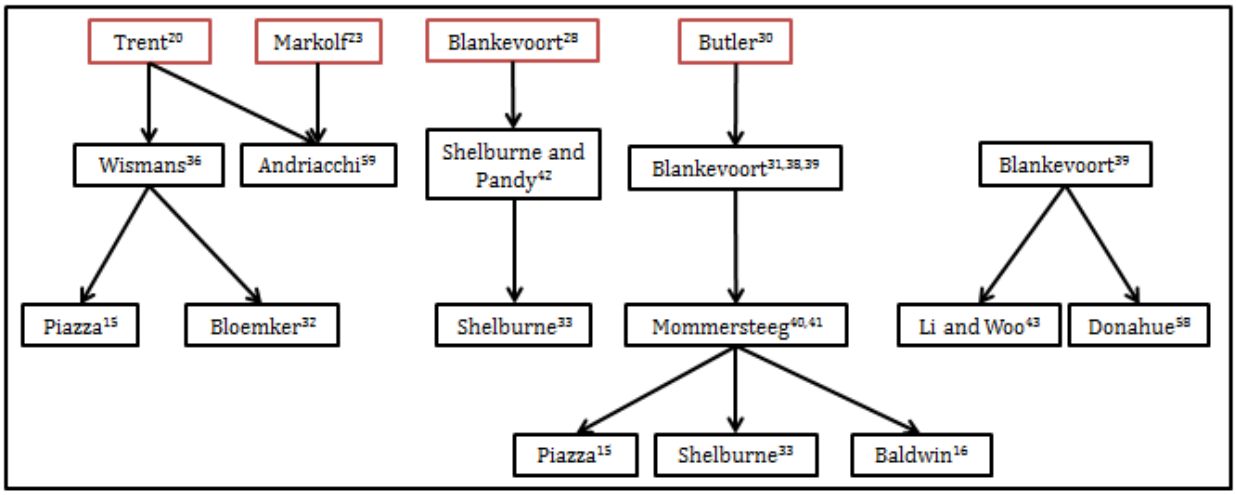

Figure 1: Flowchart of ligament stiffness properties used in simulation and model studies (black) referenced from cadaver studies (red). The study at the arrow head references study at arrow tail.

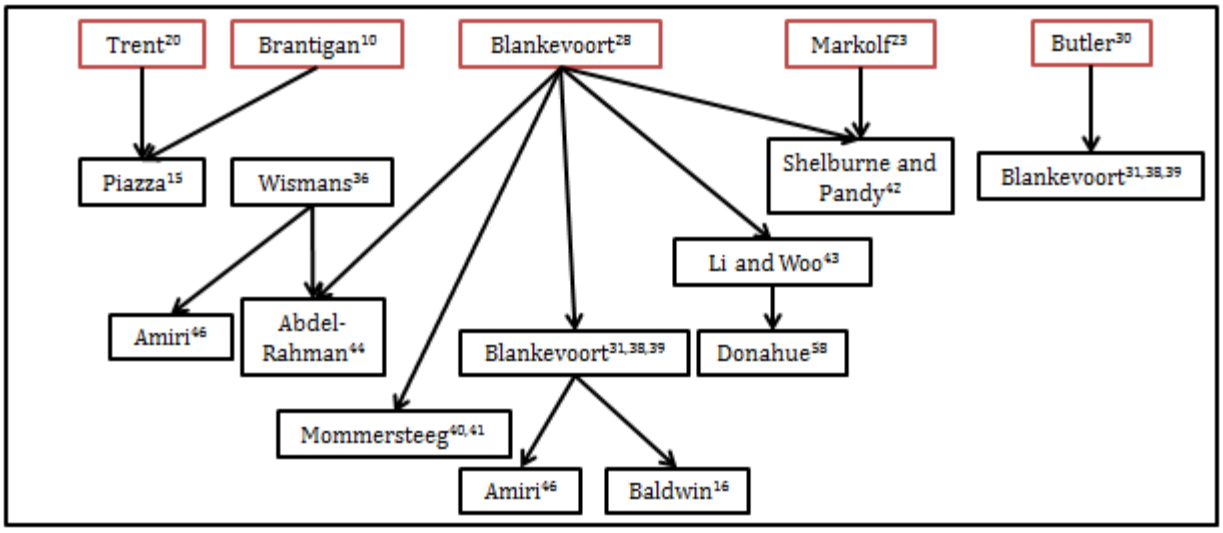

Figure 2: Flowchart of ligament length characterization used in simulation and model studies (black) referenced from cadaver studies (red). The study at the arrow head references study at arrow tail.

Table 2: Collateral ligament (MCL and LCL) and posterior capsule stiffness values reported in the reviewed literature. * indicates a cadaver study.

Study	Units	MCL	LCL	Capsule
Trent * [20]	kg/mm	7.2	6.1	-
Wismans [36]	N/mm^2	15	15	10
Andriacchi [59]	N/cm	300-500	200-500	-
Moeinzadeh [37]	N/mm^2	15	15	-
Essinger [48]	N/mm^2	15-17	18	-
Blankevoort [38]	N	2570	2000	1000
Blankevoort and Huiskes [31]	N/mm^2	2750	2000	1000
Shelburne and Pandy [42]	N/strain	2500-3000	2000	2000-4500
Abdel-Rahman [44]	N/mm	21-91	72	53-55
Li and Woo [43]	N	2750	-	1000
Piazza [15]	kN	93-97	18	-
Robinson * [27]	N/mm	42-81	-	-
Amiri [46]	N	2750	2000	1000
Shi [60]	N/mm	72	61	-
Wijdicks * [29]	N/mm	18-63	-	-
Shelburne [33]	N/strain	2500-3000	4000	3000
Baldwin [16]	N/mm	123-155	73-170	-
Bloemker [32]	N/strain	2750	2000	-

Table 3: Collateral ligament (MCL and LCL) and posterior capsule length characterization values reported in the reviewed literature. * indicates a cadaver study. SL – slack length, US – ultimate strain

Study	Units	MCL	LCL	Capsule
Wismans [36]	%	-3 - 5	5	5
Andriacchi [59]	cm	5.1 - 6.6	5.8	7.484 - 7.495
Butler * [30]	mm	-	48.7 - 50.9	-
Essinger [48]	%	1 - 4	5	-
Blankevoort [38]	strain	0.03 - 0.04	- 0.25 - 0.08	- 0.18 - 0.04
Shelburne and Pandy [42]	strain	0.02 - 0.04	0.02	0.06
Martelli [51]	mm	81	47	-
Abdel-Rahman [44]	strain	0.94 - 1.049	1.05	1.08
Quapp [26]	% - US	17.1	-	-
Li and Woo [43]	mm - SL	0.2 - 1.1	-	-
Robinson * [27]	mm	7.1 - 12.0	-	-
Amiri [46]	strain	0.05	0.18	0.03
Shelburne [33]	strain	0.044	0.056	0.064 - 0.077
Wijdicks * [29]	mm - US	2.1-8.7	-	-
Baldwin [16]	strain	0.96 - 1.04	0.96 - 1.04	-

In some studies, optimization routines are implemented to allow ligament properties (stiffness and strain) taken from cadaver studies to vary until simulated curves fit to experimental curves [16, 39, 40, 43, 47]. However, these ligament properties are optimized under a single condition (e.g., one flexion angle, constant applied load) and were not reported to be applicable at different flexion angles or in various loading conditions. However, ligament properties, like slack length should not change at varying flexion angles. The contributions of different ligaments change with varying motion or loading [28, 34], however, the material properties of ligaments do not change under different conditions [25-27, 29, 30]. In this review, no studies were found to report the difference between the material properties of the ligaments used before and after an optimization routine.

Anatomically, ligaments are overlapping sheaths of protein fibers that attach to the bones over a small area with different attachment sites (Figure 3) [61]. However, in models

used in simulations, ligaments are not typically modeled as sheaths. Rather, they are modeled as 'bands' with discrete attachment sites, instead of an area of attachment sites (Figure 4). Studies use different numbers of bands (Table 4) because it is not currently understood how different numbers of bands affect simulation outputs. Previous studies have used several methods to determine these attachment sites: measured on one cadaver [40, 46, 62], "conveniently chosen" [43, 60], or optimized across trials [16]. However, these methods for determining attachment sites cannot be easily replicated across multiple specimens or in live patients. There has not been a study to determine how small, incremental changes in ligament attachment sites affect simulation outputs.

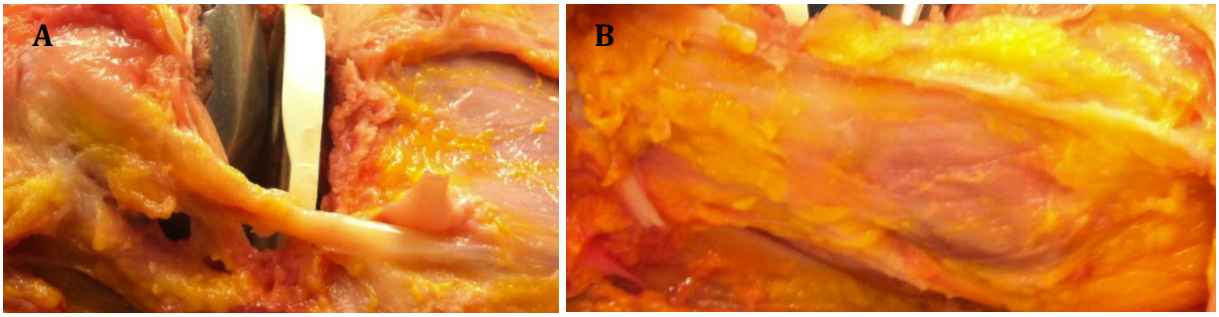

Figure 3: Dissected (A) lateral collateral ligament and (B) medial collateral ligament. The collateral ligaments are sheaths of fibers that attach to the bone over a small area.

Collateral ligament and capsule bands are also modeled in two ways: overlapping or crisscrossing bands [10, 32, 33, 35, 36, 44] and not overlapping bands [15, 16, 39, 42, 46, 47] (some studies do not clarify [43, 51, 58, 59]) (Figure 4). Overlapping bands may replicate the different anatomical structures that make up the medial collateral ligament [27, 34] and the various soft tissues of posterior capsule. However, it has not been investigated how overlapping or not overlapping the ligament bands changes the simulation kinematics and forces.

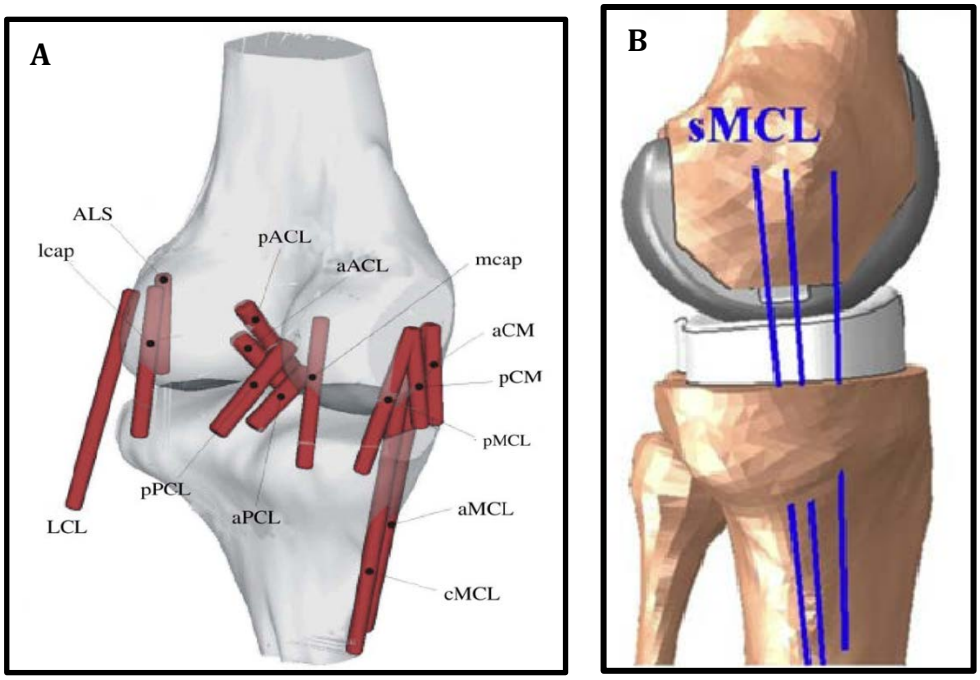

Figure 4: Ligaments are modeled in simulations as either (A) overlapping [33] or (B) not overlapping. It is not known how these different representations affect the simulation outputs.

Table 4: Number of bands to represent the collateral ligaments (MCL and LCL) and posterior capsule reported in the reviewed literature. * indicates a cadaver study.

Study	MCL	LCL	Capsule
Crowninshield [35]	3	1	4
Moeinzadeh [37]	1	1	-
Andriacchi [59]	4	3	8
Butler * [30]	2	2	2
Blankevoort [31, 38]	3	3	2
Shelburne and Pandy [42]	2	1	1
Li and Woo [43]	5	-	-
Piazza [15]	2	2	-
Donahue [58]	5	-	-
Robinson * [27]	3	-	-
Amiri [46]	3	1	4
Guess [47]	3	3	-
Bloemker [32]	3	3	-
Fitzpatrick [10]	3	3	-

2.3 Conclusion

While computer simulations of the knee joint are commonly used, there is great variability in how they are constructed. Various modeling choices that are made in creating simulations are adapted from cadaver studies or appear to be arbitrarily chosen. These modeling decisions include, but are not limited to: inclusion/exclusion of soft tissues and muscles, soft tissue and muscle properties, bone geometry, ligament wrapping and attachment sites, number of elements used to represent collateral ligaments and posterior capsule, joint contact, type of simulation (i.e., quasi-static, dynamic, finite element, lumped parameter), and simulation inputs and outputs. In this chapter, a literature review was summarized to illustrate the variability in modeling choices with regard to soft tissue properties (stiffness and slack length), attachment site, and the number of bands in existing models and simulations.

These models and simulations may closely replicate experimental motion; however the modeling choices are seemingly arbitrary. None of these studies have parametrically investigated the effect of these modeling choices on simulation outputs, and provide little support for their ligament representations. This chapter highlights the necessity of a sensitivity study to determine which modeling choices significantly affect simulation kinematics.

The research presented in the following chapters highlights how modeling parameters influence the varus-valgus rotation in a forward dynamic simulation of TKA.

Chapter 3: Methods

3.1 Cadaver Testing

The simulated motion for this study came from one cadaver specimen. The data was obtained through an NIH R21 study on 17 fresh-frozen cadavers using a custom knee stability device [13] and surgical navigation system [63-65] (Figure 5).

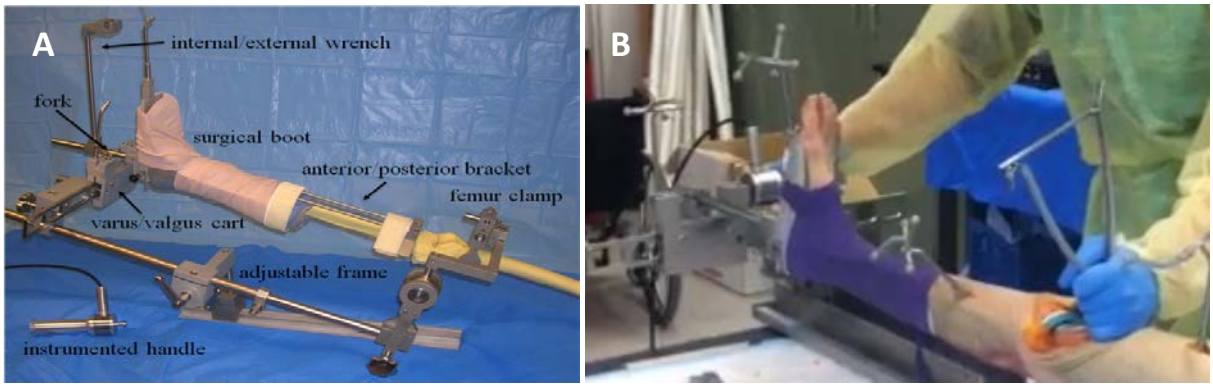

Figure 5: (A) Setup of custom knee stability device and (B) Cadaveric study of varus-valgus motion using knee stability device. A medial-lateral load is applied inferior to the specimen's ankle to produce varus-valgus rotation at the knee. Optical trackers are used to record relative motions of the stability device and bones to determine varus-valgus rotation. The testing was done after the specimen underwent a TKA.

The cadaveric specimen underwent the following testing procedure. The experimental setup was calibrated to establish reference frames in space. An experienced orthopedic surgeon (Dr. Jeffrey Granger) attached optical trackers to the specimen's femur and tibia. The surgeon located and recorded bony landmarks on the specimen's leg using a surgical probe [66]. The custom surgical navigation system [67] relates the position and orientation of the optical trackers to the bony landmarks to establish anatomical reference frames [65]. Optical trackers were also attached to the surgical boot and varus-valgus cart (Figure 5) and the surgeon located points on the stability device that were used to establish reference frames for the boot and varus-valgus cart. Once the system was calibrated, the navigation system

recorded the motions of the optical trackers attached to the femur, tibia, surgical boot, and varus-valgus cart during all testing [13].

Before the TKA was performed, preoperative testing was done to determine the stability of the native joint. The specimen's foot was placed in the surgical boot, and into the varus-valgus cart (Figure 1). The custom stability device was used to test varus-valgus rotation, internal-external rotation, and anterior-posterior displacement in response to applied loads at 0° and 20° of knee flexion [13].

The surgeon then performed a posterior-stabilizing total knee replacement using the Zimmer Nexgen LPS flex product line. The component sizes used for the specimen were determined by the surgeon (Table 5).

Table 5: Component and polyethylene insert sizes used for the cadaveric specimens in this study. These sizes were determined by the orthopedic surgeon during surgery.

Femur	Poly (mm)	Tibial tray
G	10	7

Following component implantation, the joint was again tested using the custom stability device. This research specifically focuses on the varus-valgus rotation of a TKA joint. The specimen's leg was placed in the stability device and an instrumented handle with a load cell was used to manually apply loads medially and laterally to the varus-valgus cart along a track inferior to the specimen's ankle (Figure 5) [13]. Using the Grood and Suntay convention [68], varus-valgus rotation of the knee was calculated based on the motion of the optical trackers attached to the specimen's femur and tibia. Varus-valgus motion was studied because it directly applies force to the collateral ligaments and is currently considered by surgeons to determine stability in the knee during TKA [13]. All initial testing was done with component and

polyethylene insert sizes chosen by the surgeon (Table 5). A second polyethylene insert two millimeters larger was also used for testing. In total, four sets of varus-valgus data were collected (two sizes of the polyethylene insert at 0° and 20° of knee flexion).

After testing, the components were removed and an instrumented plate was used to measure the orientations of the bone cuts on the femur and tibia [66]. The cuts were recorded to determine the placement of the femoral and tibial components on the femur and tibia, respectively.

3.2 The Varus-Valgus Simulation

This research used a forward-dynamic simulation developed by Ph.D. candidate Joseph Ewing (Neuromuscular Biomechanics Lab, The Ohio State University) in collaboration with Dr. Stephen Piazza (The Pennsylvania State University) as part of an NIH R21 grant for the development of subject-specific simulations of TKA. The varus-valgus simulation replicates the varus-valgus motion from the cadaver study (Figure 6). The applied force and tracked motion of the femur are used as inputs to the simulation.

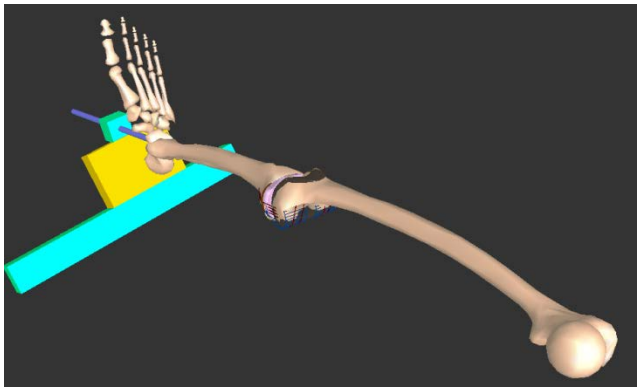

Figure 6: Full view of varus-valgus simulation. The simulation includes bones, femoral and tibial components, polyethylene insert, and the knee stability device.

The simulation was created through SIMM Dynamics Pipeline (MusculoGraphics, Inc.; Santa Rosa, CA, USA) and SD/FAST (Parametric Technologies; Needham, MA, USA) and is a

forward dynamic, lumped parameter model of the TKA joint [15, 69]. The simulation includes rigid body models of the femur, tibia, fibula, foot, femoral component, and tibial component (Figure 6). The femoral and tibial components are rigidly attached to the bones and contact between the components excludes friction. The contact forces between the polyethylene insert and the femoral component are determined with a rigid-body-spring model (RBSM) [70]. The RBSM contact force depends on angle of contact between surfaces. The model in the simulation does not include any muscles.

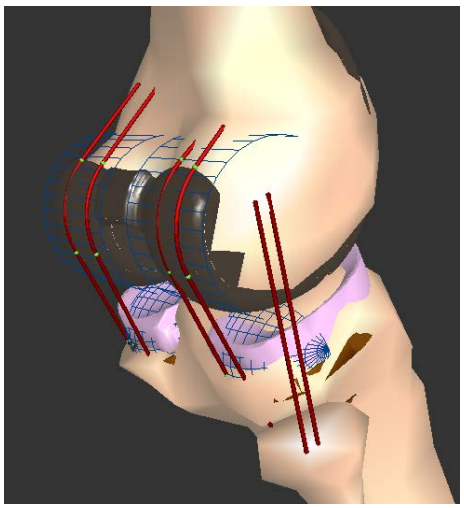

Figure 7: Posterior-lateral view of the knee model used in the simulation. The collateral ligaments and posterior capsule are modeled as bands (red). The femoral (gray) and tibial components (hidden) are rigidly attached to the distal and proximal ends of the bones, respectively. The polyethylene insert (pink) rigidly attaches to the tibial component and makes spring contact with the femoral component. The wrapping surfaces (blue) guide the ligaments along the contours of the components and bony surfaces.

The model includes the medial and lateral collateral ligaments and posterior capsule. The ligaments are described by quadratic spring force/deformation curves [15]. The cruciate ligaments are not included because they sacrificed during surgery. The implant used is a posterior (cruciate ligament) substituting component and the anterior cruciate ligament is removed. Each collateral ligament is modeled by two bands. The posterior capsule is modeled by four bands (two medial and two lateral bands) (Figure 7). The ligaments have discrete,

arbitrarily chosen attachment points to the bones [15] and conform to wrapping surfaces that mimic bony landmarks and the contours of the components.

The model used in the simulation was made specimen-specific by scaling the bones and aligning the components based on measurements from the cadaver study. For each specimen, proximal-distal and medial-lateral scale factors were determined based on the bony landmarks recorded using the surgical probe before the TKA. The generic femur and tibia bone models were scaled to be closer approximations of the size of the specimen bone [71]. The components were aligned to the bones in the orientations specified by the bone cuts (recorded using the instrumented plate). The models for different component sizes were created by Dr. Piazza and specified for each specimen (Table 5).

The simulation outputs angles (varus-valgus, internal-external), displacements (anterior-posterior), and ligament and contact forces at each time step of 0.05 seconds.

3.3 Ligament Property Optimization

After calculating the varus-valgus rotation angles, scaling the bones, and aligning the components to the bones, the final step for preprocessing the cadaver motion was to estimate initial slack lengths before any force was applied to the instrumented handle. An optimization routine (developed by Joseph Ewing) with a gravity-only simulation was used to estimate the slack lengths of the LCL, MCL, and posterior capsule without any load applied. The gravity-only simulation modeled the leg as resting in the stability device at 0° and 20° of knee flexion, with no loads acting on the leg other than gravity. The optimization adjusted the ligament slack lengths and stiffness values to minimize the difference between simulated and experimental rotations (varus-valgus, internal-external), and translations (anterior-posterior) with the two

sizes of polyethylene inserts, at 0° and 20° of knee flexion. Four simulations are used in the optimization routine to represent the different testing conditions (Table 6).

Table 6: Four conditions were used in the optimization routine to estimate initial slack lengths for each specimen. The 10 mm polyethylene insert was the size chosen by the surgeon.

Knee flexion angle	Polyethylene insert
0°	10 mm
0°	12 mm
20°	10 mm
20°	12 mm

The initial slack lengths for the specimen (Table 7) used in this study were estimated using this optimization routine.

Table 7: Optimized ligament slack lengths for the LCL and MCL. These slack lengths were the initial values used in this study.

Initial ligament length (cm)			
Anterior LCL	Posterior LCL	Anterior MCL	Posterior MCL
4.89	4.78	7.27	8.72

3.3 Sensitivity Analysis

This research investigated the relative changes in knee laxity in simulations of varus-valgus motion in response to incremental changes in modeling choices. The ligament properties and modeling parameters altered were slack length, stiffness, attachment site, and number of bands.

The model discussed above has been used previously in simulations of TKA [15, 69]. For the purposes of this thesis, the model was considered the “two band” or original model because the collateral ligaments were each represented with two bands (Figure 8, A) [15, 69]. A “four band” model was adapted from the two band model by including an additional two bands for each of the collateral ligaments (Figure 8, B). One of the two additional bands was placed equidistant between the two existing bands in the original (two band) model. A second

band was added either more anteriorly than the original anterior band (Figure 9, A) or more posteriorly than the original posterior band (Figure 9, B). The additional bands were only added to one collateral ligament at a time.

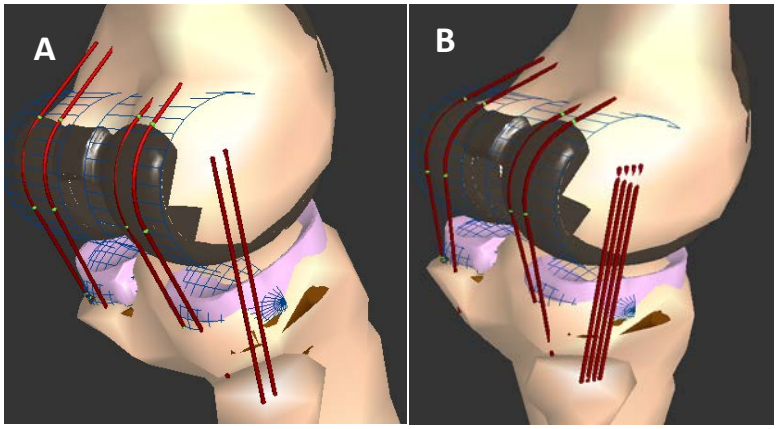

Figure 8: Posterior-lateral views of the LCL for the two (A) and four (B) band models.

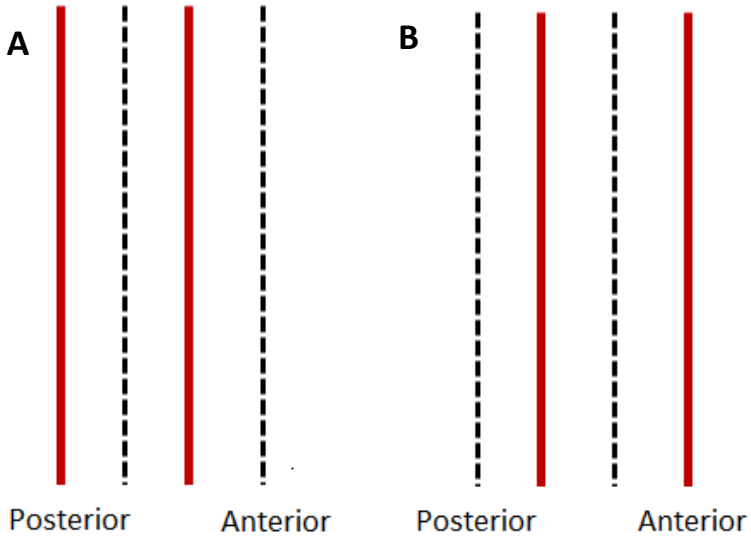

Figure 9: Lateral view of the LCL (right leg model). Additional bands (black dashed) were added to the two band model (red) in two ways: more anterior bands (A) and more posteriorly bands (B).

The material properties of the additional bands were dependent on the location of the new bands and the material properties of the original bands. In the original model, the stiffness of the posterior band of the MCL contained 2/3 of the combined stiffness of the ligament [15, 69]. In the four band model, 2/3 of the original stiffness was divided evenly between the two

most posterior bands and the remaining 1/3 of the original stiffness was divided evenly between the two most anterior bands. Therefore, the overall stiffness of the MCL did not change from the two band to four band model. The variable names and equations to determine slack length in the four band model can be found in Tables 8 and 9.

Table 8: Definitions used for determining slack length of bands in the four band model

Description	Definition
Slack length	l
Slack length of anterior band	l_{ant}
Slack length of posterior band	l_{pos}
Average slack length of bands in the two band model	$l_{avg} = \frac{l_{ant} + l_{pos}}{2}$
Difference between anterior and posterior slack length in the two band model	$l_{diff} = l_{pos} - l\_ant$

Table 9: Definitions used to determine slack length of MCL bands in the four band model

Band position	More anterior bands	More posterior bands
Most anterior band	$l = l_{ant} - l_{diff}$	$l = l_{ant}$
Second most anterior band	$l = l_{ant}$	$l = l\_avg$
Second most posterior band	$l = l\_avg$	$l = l_{pos}$
Posterior band	$l = l_{pos}$	$l = l_{pos} + l_{diff}$

Table 10: Slack length values used in simulations to analyze sensitivity of change ligament slack length

	Slack Length (cm)				
Band	**Optimized Values**	**+2.5%**	**-2.5%**	**+5%**	**-5%**
Anterior LCL	4.89	5.01	4.77	5.14	4.65
Posterior LCL	4.78	4.90	4.66	5.02	4.54
Anterior MCL	7.27	7.46	7.09	7.64	6.91
Posterior MCL	8.72	8.94	8.50	9.16	8.28
Posterior capsule 1	8.87	9.10	8.65	9.32	8.43
Posterior capsule 2	9.48	9.72	9.25	9.96	9.01
Posterior capsule 3	8.10	8.30	7.90	8.50	7.69
Posterior capsule 4	7.52	7.71	7.33	7.89	7.14

Table 11: Stiffness values used in simulations to analyze sensitivity of change ligament stiffness

	Stiffness (kN)						
Band	**Optimized Values**	**+25%**	**-25%**	**+50%**	**-50%**	**+75%**	**-75%**
Anterior LCL	18.66	23.32	13.99	27.99	9.33	32.65	46.67
Posterior LCL	12.03	15.03	9.02	18.04	6.01	21.04	30.06
Anterior MCL	71.79	89.74	53.84	107.69	35.90	125.64	17.95
Posterior MCL	106.26	132.82	79.69	159.39	53.13	185.95	26.57
Posterior capsule 1	26.09	32.61	19.57	39.14	13.05	45.66	6.52
Posterior capsule 2	16.28	20.35	12.21	24.42	8.14	28.49	4.07
Posterior capsule 3	19.45	24.31	14.59	29.17	9.72	34.03	4.86
Posterior capsule 4	22.12	27.64	16.59	33.17	11.06	38.70	5.53

A sensitivity analysis of the two band and four band models was conducted. “Two band” sensitivity was defined when the MCL and LCL were each represented by two bands (Figure 8, A) and “four band” sensitivity was defined when either the MCL or LCL was represented by four bands (Figure 8, B).

Ligament slack length and stiffness were altered in the two band model with the knee at 0° and 20° knee flexion on a global, ligament, and band level. The global level was defined as an adjustment to all bands of all ligaments surrounding the knee (collateral ligaments and posterior capsule). The ligament level was defined as an adjustment to both bands of one collateral ligament (MCL, LCL). The band level was defined as an adjustment to only one band of one ligament (anterior and posterior bands of the MCL and LCL). The slack length was altered by ±2.5% and ±5% of the optimized values (Table 10). An increase in slack length (+2.5% and +5% of the optimized value) was equivalent to a longer ligament and a decrease in slack length (-2.5% and -5% of the optimized value) was equivalent to a shorter ligament. Ligament stiffness was altered by ±25%, 50%, and 75% of the optimized values (Table 11). An increase in stiffness (+25%, +50%, and +75%) was equivalent to a tighter ligament and a decrease in stiffness (-25%, -50%, and -75%) was equivalent to a looser ligament.

The simulation sensitivity to translated ligament attachment sites was investigated at 0º and 20º knee flexion in the two band model. Translating attachment sites was accomplished by moving the location of the ligament's attachment sites to the bone by 1 cm in the anterior, posterior, superior, and inferior anatomical directions. Both bands of the ligament were translated together, and only one ligament was altered at a time.

The attachment sites of the ligament bands were altered to create different band configurations. The original (two band) model arranged the bands of each ligament such that they were nearly parallel in the sagittal plane [15, 69]. An "X configuration" was defined when the locations of either the femoral or tibial attachment sites of one ligament were switched to create an "X" configuration (Figure 10). The ligament properties (slack length) were not adjusted because the length of each band was much longer than the distance between the attachment sites of the two bands. The "X" configuration was investigated in the two band model at 0º and 20º knee flexion.

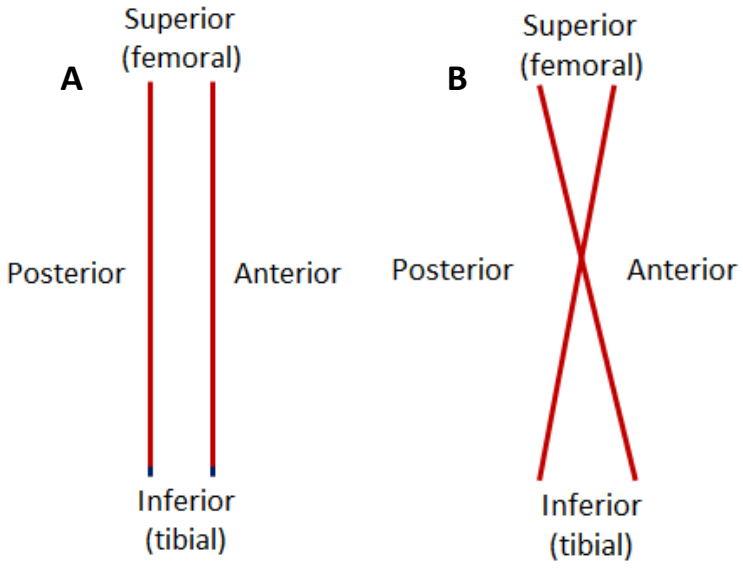

Figure 10: Original (A) and altered (B) arrangement of the anterior and posterior bands of the LCL. The femoral attachment site was the attachment site of the ligament to the femur and the tibial attachment site was the attachment site of the ligament to the tibia.

Finally, the impact of adding bands to the collateral ligaments was investigated with the two band model at 0º and 20º knee flexion. The results of adding bands in the two locations described above and the results of a modeling literature review encouraged further study on the configuration of the bands of the MCL.

The four band model was used to analyze the simulation sensitivity to 16 arrangements of the four bands of the MCL. In each arrangement, the two most anterior and two most posterior bands joined at one attachment site to form a "V" shape. Four categories of arrangements were constructed, simulated, and categorized based on the point of view were a "V" could be recognized.

- Tibial (Figure 11): The "V" appears upright from the point of view of the tibia.
- Femoral (Figure 12): The "V" appears upright from the point of view of the femur.
- Anterior (Figure 13)Figure 12: The "V" appears upright in the two most anterior bands.
- Posterior fans (Figure 14): The "V" appears upright in the two most posterior bands.

The naming convention of simulations in each of the four categories was the same (Figures 11, 12, 13, 14). The first word denoted the direction (anterior or posterior) towards which the two most anterior bands (anterior group) were moved. The second word denoted the direction in which the two most posterior bands (posterior group) were moved. No adjustments were made to the slack lengths of any bands.

- Anterior/anterior (A): Both the anterior group and the posterior group meet at a more anterior attachment site (along the more anterior band of each group).
- Anterior/posterior (B): The anterior group meets at a more anterior attachment site (along the most anterior band). The posterior group meets at a most posterior attachment site (along the most posterior band).
- Posterior/anterior (C): The anterior group meets at a more posterior attachment site (along the more posterior band of the anterior group). The posterior group meets at a most anterior attachment site (along the more anterior band of the posterior group).
- Posterior/posterior (D): Both the anterior group and the posterior group meet at a more posterior attachment site (along the more posterior band of each group).

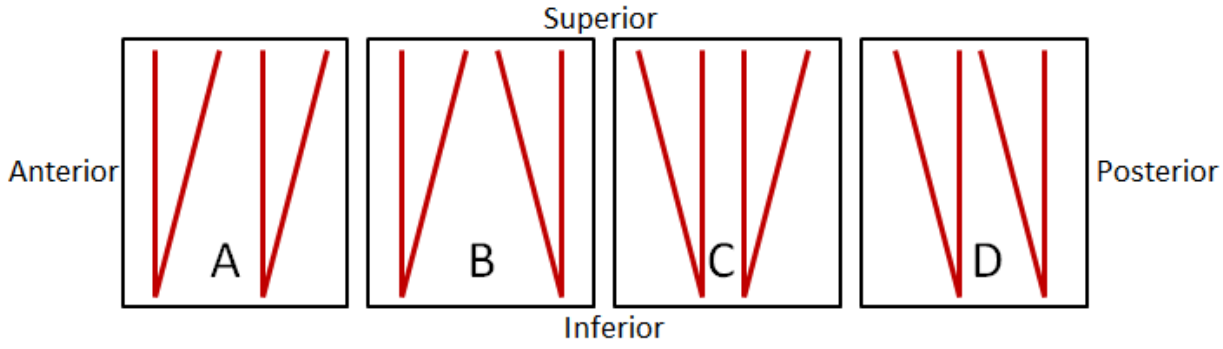

Figure 11: Tibial fans of the MCL (A) anterior/anterior (B) anterior/posterior (C) posterior/anterior (D) posterior/posterior

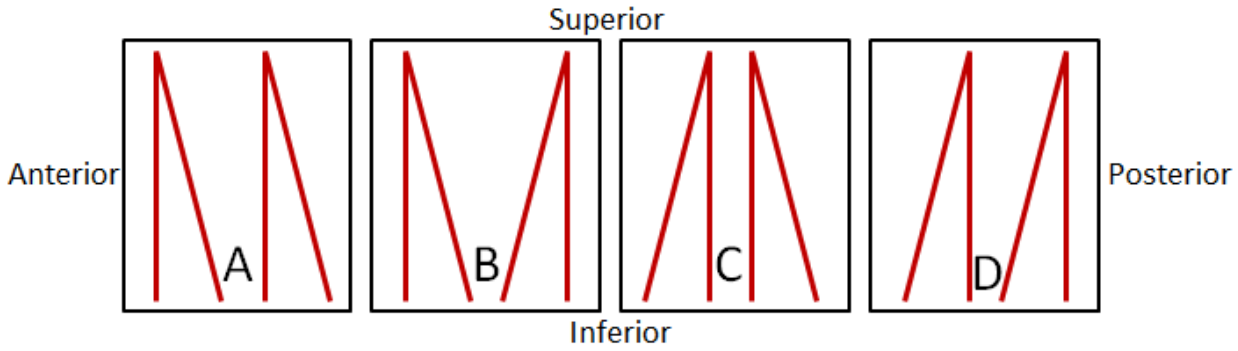

Figure 12: Femoral fans of the MCL (A) anterior/anterior (B) anterior/posterior (C) posterior/anterior (D) posterior/posterior

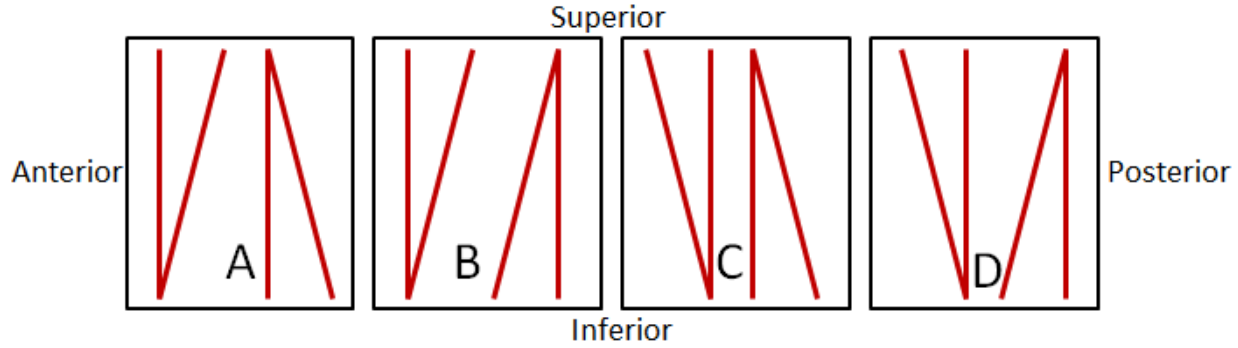

Figure 13: Anterior fans of the MCL (A) anterior/anterior (B) anterior/posterior (C) posterior/anterior (D) posterior/posterior

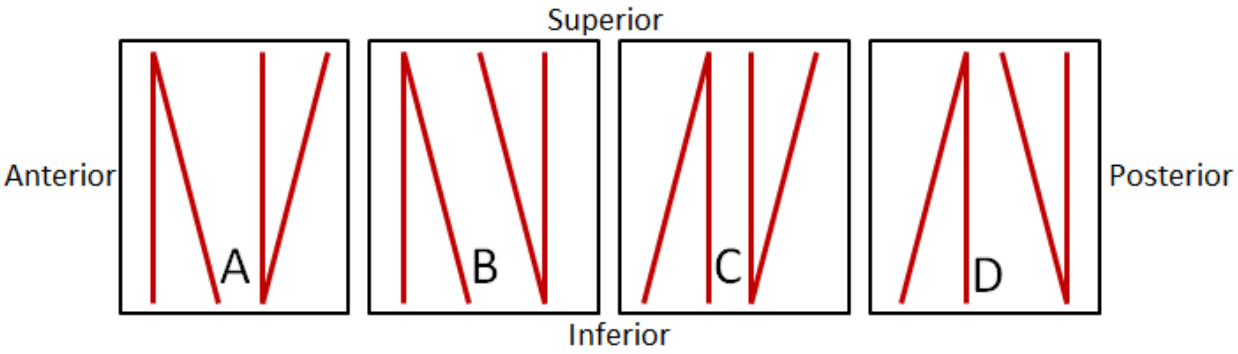

Figure 14: Posterior bands of the MCL (A) anterior/anterior (B) anterior/posterior (C) posterior/anterior (D) posterior/posterior

Chapter 4: Results

A total of 850 simulations were run to determine the simulation sensitivity to incremental changes in ligament properties. All simulations were compared to a baseline or unaltered simulation which is listed in each section. An applied force versus varus-valgus curve was calculated from the output of each simulation (Figure 15) and fit to a third order polynomial. From this curve, the laxity (the amount of varus-valgus rotation) under ±40 N loads at 0° knee flexion and ±15 N loads at 20° knee flexion was calculated. A change in laxity was calculated as the absolute difference in laxity between each altered simulation and a baseline, or unaltered, simulation (Δ Laxity). A change in laxity of zero indicated no difference between the varus-valgus rotation of the baseline simulation and the altered simulation. The most varus and most valgus angles of each simulation were also compared to the baseline simulation (ΔVarus, ΔValgus).

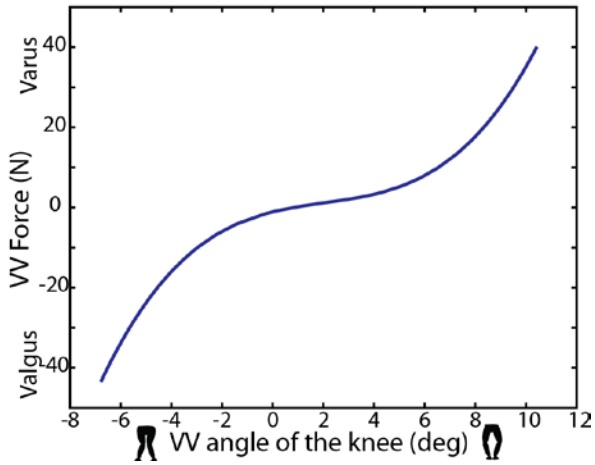

Figure 15: Sample force versus varus-valgus curve

Increasing or decreasing the slack length of any ligament by less than 5% of the optimized value increased or decreased (respectively) joint laxity. Increasing or decreasing the stiffness of any ligament only affected the joint laxity when altered by at least 50% of the optimized value. Translating attachment sites or creating an "X" configuration with ligament

band did not change joint laxity. Increasing the number of bands used to represent the MCL affected joint laxity and suggested sensitivity to the anterior-posterior location of additional bands. Valgus rotation increased when more anterior bands represented the MCL at both 0° and 20° knee flexion. In contrast, valgus rotation decreased at 0° knee flexion and increased and decreased at 20° knee flexion when more posterior bands represented the MCL.

4.1 Two Band Model Sensitivity

The baseline simulation in the following section was the two band model [15, 69] with optimized slack length and stiffness values (black curve in each figure).

4.1.1 Slack length

Small changes (±2.5% and ±5% of the optimized value) in slack length caused noticeable differences in the simulated varus-valgus rotation and laxity of the joint.

a. Global level

Globally increasing slack length changed joint laxity more than globally decreasing slack length at 0^{o} knee flexion. In contrast, globally decreasing slack length changed laxity more than globally increasing slack length at 20^{o} knee flexion. Globally changing slack length affected the valgus rotation more than the varus rotation of the joint at both knee flexion angles.

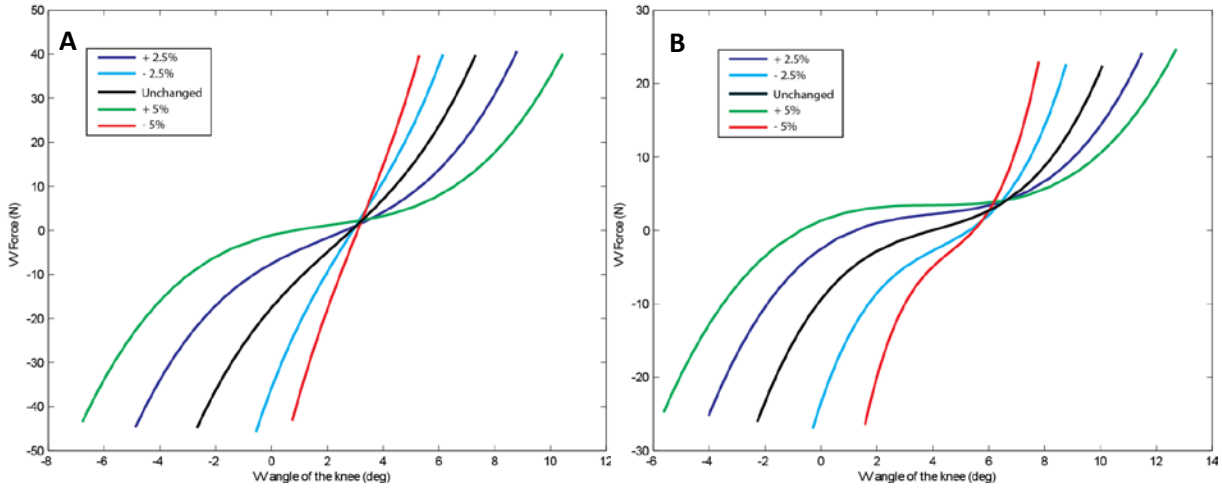

Figure 16: Global level slack length simulations (A) 0° and (B) 20° knee flexion

Table 12: Global level slack length simulations, 0° knee flexion

Simulation	Laxity (º)	Δ Laxity (º)	ΔVarus (º)	Δ Valgus (º)
Minus 5%	4.41	5.16	1.95	3.21
Minus 2.5%	6.39	3.18	1.10	2.08
Unchanged	9.57	-	-	-
Plus 2.5%	13.12	3.55	1.28	2.26
Plus 5%	16.78	7.21	2.91	4.30

Table 13: Global level slack length simulations, 20° knee flexion

Simulation	Laxity (º)	Δ Laxity (º)	ΔVarus (º)	Δ Valgus (º)
Minus 5%	4.82	4.61	1.48	3.13
Minus 2.5%	6.89	2.54	0.76	1.78
Unchanged	9.57	-	-	-
Plus 2.5%	11.42	1.99	0.40	1.59
Plus 5%	12.79	3.36	0.56	2.81

b. Ligament level

Decreasing the slack length of the LCL changed laxity more than increasing the slack length of the LCL at 0º and 20° knee flexion. Increasing or decreasing the slack length of the LCL only affected the varus rotation of the joint. Increasing or decreasing the slack length of the MCL changed laxity more than increasing or decreasing the slack length of the LCL at both knee flexion angles. Decreasing the slack length of the MCL affected both the varus and valgus

rotations of the joint, while increasing the slack length of the MCL only affected the valgus rotation of the knee.

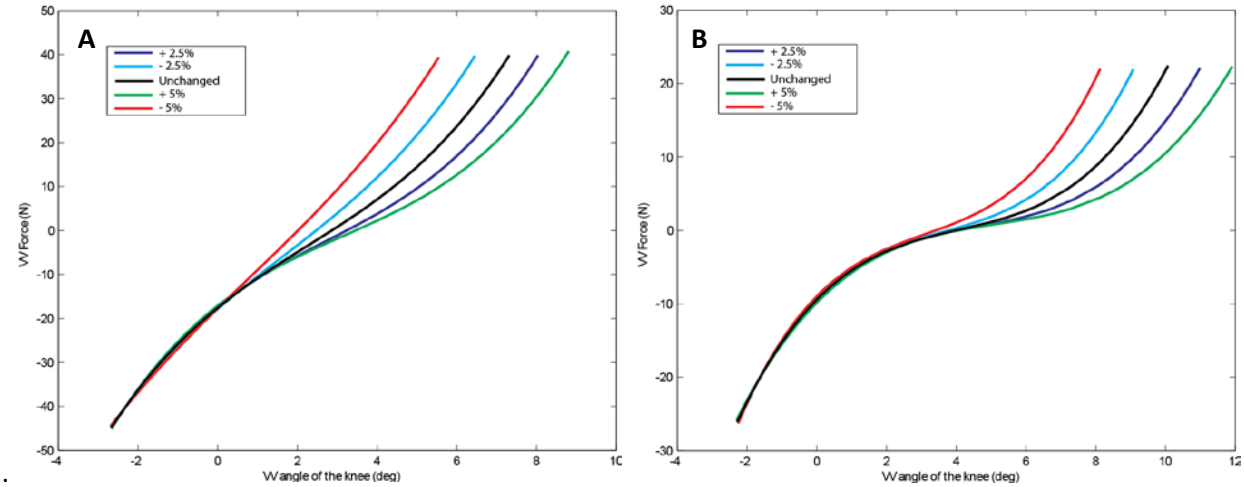

Figure 17: LCL ligament level slack length simulations (A) 0° (B) 20° knee flexion

Table 14: LCL ligament level slack length simulations, 0° knee flexion

Simulation	Laxity (º)	Δ Laxity (º)	ΔVarus (º)	Δ Valgus (º)
Minus 5%	7.83	1.74	1.69	0.05
Minus 2.5%	8.72	0.86	0.83	0.03
Unchanged	9.57	-	-	-
Plus 2.5%	10.28	0.71	0.69	0.02
Plus 5%	10.99	1.42	1.38	0.04

Table 15: LCL ligament level slack length simulations, 20° knee flexion

Simulation	Laxity (º)	Δ Laxity (º)	ΔVarus (º)	Δ Valgus (º)
Minus 5%	7.93	1.50	1.65	0.15
Minus 2.5%	8.73	0.70	0.79	0.10
Unchanged	9.57	-	-	-
Plus 2.5%	10.15	0.72	0.79	0.07
Plus 5%	10.81	1.38	1.54	0.16

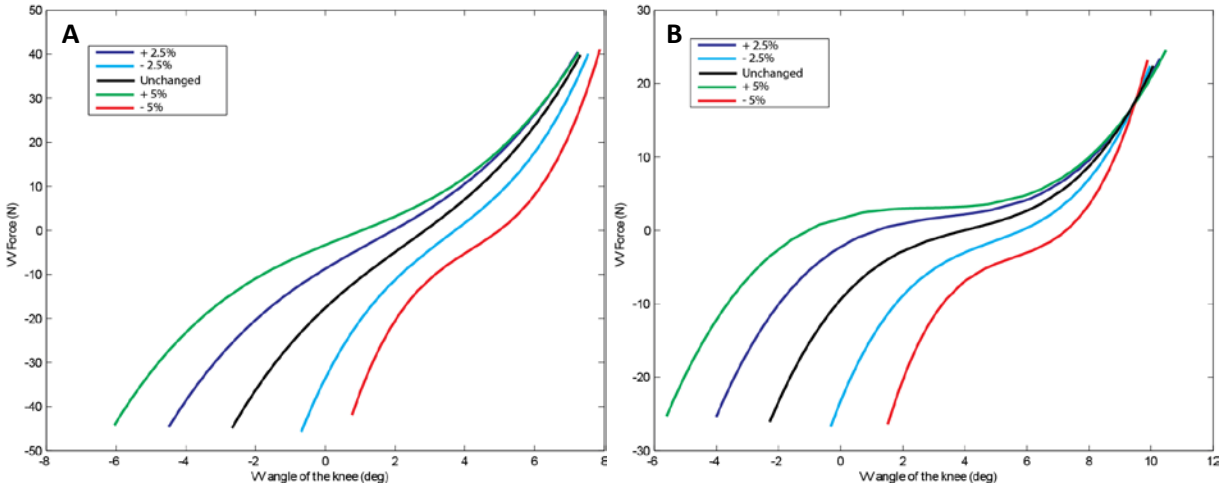

Figure 18: MCL ligament level slack length simulations (A) 0° and (B) 20° knee flexion

Table 16: MCL ligament level slack length simulations, 0° knee flexion

Simulation	Laxity (º)	Δ Laxity (º)	ΔVarus (º)	Δ Valgus (º)
Minus 5%	6.79	2.78	0.37	3.15
Minus 2.5%	7.88	1.69	0.23	1.92
Unchanged	9.57	-	-	-
Plus 2.5%	11.23	1.66	0.17	1.83
Plus 5%	12.83	3.26	0.19	3.45

Table 17: MCL ligament level slack length simulations, 20° knee flexion

Simulation	Laxity (º)	Δ Laxity (º)	ΔVarus (º)	Δ Valgus (º)
Minus 5%	6.42	3.01	0.54	3.55
Minus 2.5%	7.82	1.61	0.27	1.88
Unchanged	9.57	-	-	-
Plus 2.5%	10.69	1.26	0.45	1.71
Plus 5%	11.49	2.06	1.04	3.10

c. Band level

Increasing or decreasing the slack length of the anterior band of the LCL changed joint laxity more than increasing or decreasing the slack length of the posterior band at both 0° and 20° knee flexion. For both bands of the LCL, decreasing slack length of the band resulted more change laxity compared to increasing the slack length of the band. Increasing or decreasing the slack length of either band of the LCL only affected the varus rotation of the knee.

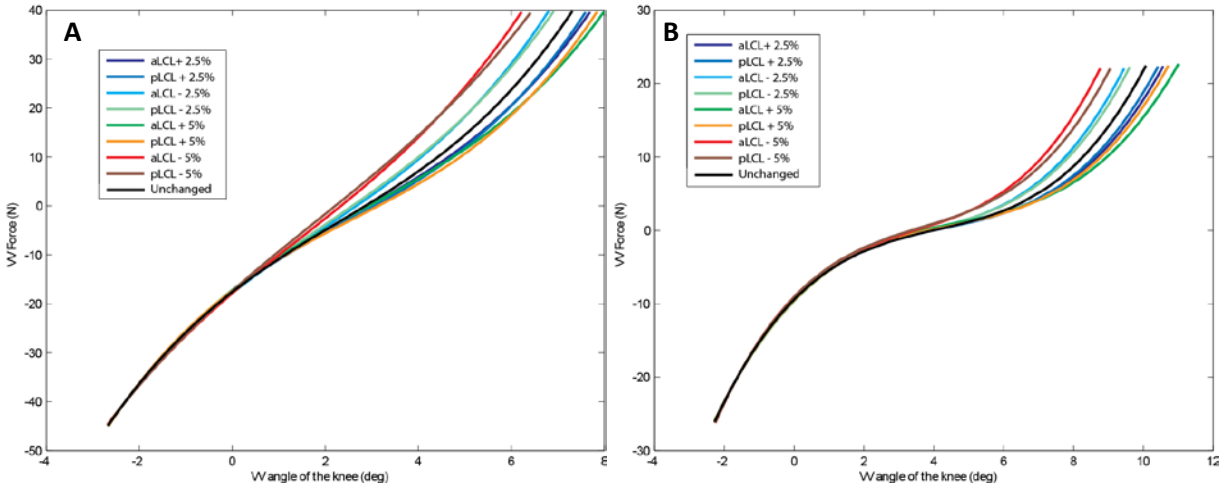

Figure 19: LCL band level slack length simulations (A) 0° and (B) 20° knee flexion

Table 18: Anterior LCL band level slack length simulations, 0° knee flexion

Simulation	Laxity (º)	Δ Laxity (º)	ΔVarus (º)	Δ Valgus (º)
Minus 5%	8.49	1.08	1.05	0.03
Minus 2.5%	9.06	0.51	0.50	0.01
Unchanged	9.57	-	-	-
Plus 2.5%	9.97	0.40	0.39	0.01
Plus 5%	10.29	0.72	0.71	0.01

Table 19: Anterior LCL band level slack length simulations, 20° knee flexion

Simulation	Laxity (º)	Δ Laxity (º)	ΔVarus (º)	Δ Valgus (º)
Minus 5%	8.46	0.97	1.12	0.16
Minus 2.5%	9.00	0.43	0.49	0.06
Unchanged	9.57	-	-	-
Plus 2.5%	9.82	0.39	0.40	0.00
Plus 5%	10.10	0.67	0.66	0.01

Table 20: Posterior LCL band level slack length simulations, 0° knee flexion

Simulation	Laxity (º)	Δ Laxity (º)	ΔVarus (º)	Δ Valgus (º)
Minus 5%	8.72	0.85	0.81	0.04
Minus 2.5%	9.18	0.39	0.38	0.02
Unchanged	9.57	-	-	-
Plus 2.5%	9.86	0.29	0.28	0.01
Plus 5%	10.11	0.53	0.52	0.02

Table 21: Posterior LCL band level slack length simulations, 20° knee flexion

Simulation	Laxity (º)	Δ Laxity (º)	ΔVarus (º)	Δ Valgus (º)
Minus 5%	8.69	0.74	0.91	0.17
Minus 2.5%	9.11	0.32	0.39	0.07
Unchanged	9.57	-	-	-
Plus 2.5%	9.71	0.28	0.30	0.02
Plus 5%	9.91	0.48	0.50	0.01

Increasing or decreasing the slack length of the anterior band of the MCL changed laxity more than increasing or decreasing the slack length of the posterior band of the MCL at both knee flexion angles. For both bands of the MCL, decreasing the slack length of the band changed laxity more than increasing the slack length of the band. Changing the slack length of the anterior band of the MCL affected both the varus and valgus rotations of the knee, while changing the slack length of the posterior band affected only the valgus rotation of the joint.

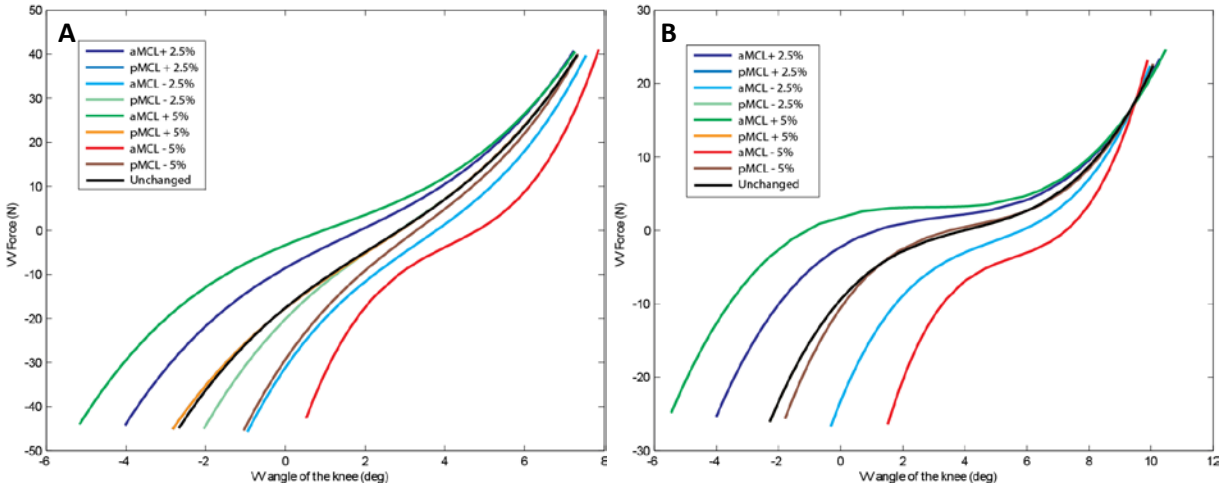

Figure 20: MCL band level slack length simulations (A) 0° and (B) 20° knee flexion

Table 22: Anterior MCL band level ligament slack length simulations, 0° knee flexion

Simulation	Laxity (º)	Δ Laxity (º)	ΔVarus (º)	Δ Valgus (º)
Minus 5%	7.01	2.56	0.36	2.92
Minus 2.5%	8.11	1.46	0.24	1.71
Unchanged	9.57	-	-	-
Plus 2.5%	10.85	1.28	0.16	1.44
Plus 5%	12.07	2.50	0.13	2.63

Table 23: Anterior MCL band level slack length simulations, 20 °knee flexion

Simulation	Laxity (º)	Δ Laxity (º)	ΔVarus (º)	Δ Valgus (º)
Minus 5%	6.42	3.01	0.54	3.55
Minus 2.5%	7.82	1.61	0.27	1.88
Unchanged	9.57	-	-	-
Plus 2.5%	10.69	1.26	0.45	1.71
Plus 5%	11.46	2.03	1.03	3.07

Table 24: Posterior MCL band level slack length simulations, 0° knee flexion

Simulation	Laxity (º)	Δ Laxity (º)	ΔVarus (º)	Δ Valgus (º)
Minus 5%	8.08	1.49	0.08	1.58
Minus 2.5%	9.03	0.55	0.04	0.59
Unchanged	9.57	-	-	-
Plus 2.5%	9.69	0.12	0.01	0.11
Plus 5%	9.69	0.12	0.01	0.11

Table 25: Posterior MCL band level slack length simulations, 20° knee flexion

Simulation	Laxity (º)	Δ Laxity (º)	ΔVarus (º)	Δ Valgus (º)
Minus 5%	9.23	0.20	0.01	0.19
Minus 2.5%	9.43	0.00	0.00	0.00
Unchanged	9.57	-	-	-
Plus 2.5%	9.43	0.00	0.00	0.00
Plus 5%	9.43	0.00	0.00	0.00

4.1.2 Stiffness

Only large changes (±25%, ±50%, ±75% of the optimized values) in stiffness caused noticeable differences in the simulated varus-valgus rotation of the joint.

a. Global

Globally decreasing the stiffness changed joint laxity more than globally increasing the stiffness at both 0° and 20° knee flexion.

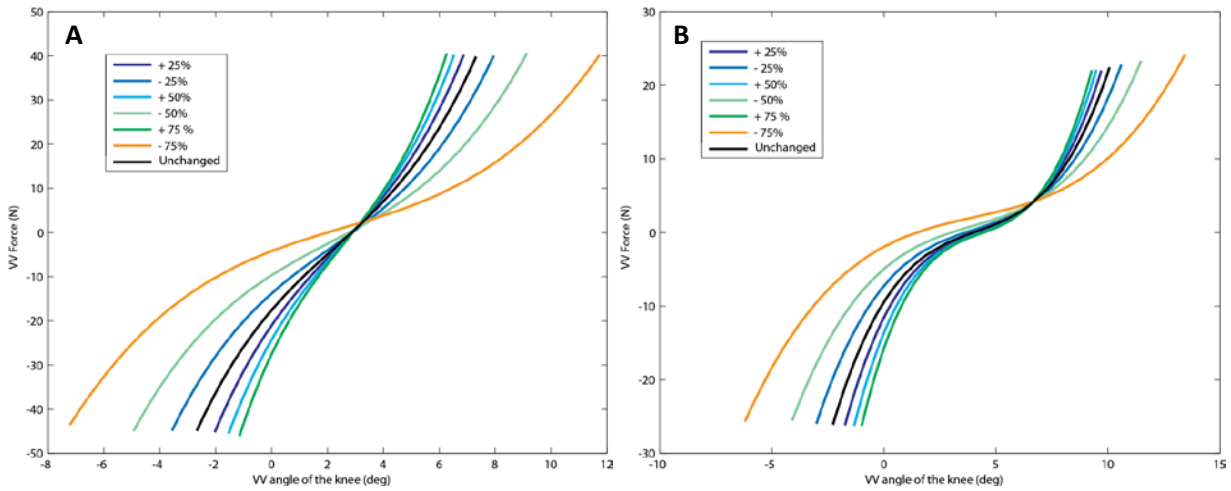

Figure 21: Global level stiffness simulations (A) 0° and (B) 20° knee flexion

Table 26: Global level stiffness simulations, 0° knee flexion

Simulation	Laxity (º)	Δ Laxity (º)	ΔVarus (º)	Δ Valgus (º)
Minus 75%	18.57	9.00	4.45	4.54
Minus 50%	13.47	3.90	1.70	2.20
Minus 25%	11.02	1.45	0.57	0.87
Unchanged	9.57	-	-	-
Plus 25%	8.49	1.08	0.45	0.64
Plus 50%	7.67	1.90	0.78	1.12
Plus 75%	7.02	2.55	1.05	1.50

Table 27: Global level stiffness simulations, 20° knee flexion

Simulation	Laxity (º)	Δ Laxity (º)	ΔVarus (º)	Δ Valgus (º)
Minus 75%	13.59	4.16	1.42	2.74
Minus 50%	11.41	1.99	0.67	1.32
Minus 25%	10.21	0.78	0.26	0.52
Unchanged	9.57	-	-	-
Plus 25%	8.87	0.56	0.18	0.38
Plus 50%	8.45	0.98	0.32	0.66
Plus 75%	8.11	1.32	0.43	0.89

b. Ligament level

Decreasing the stiffness changed laxity more than increasing the stiffness for both the LCL and MCL at 0° and 20° knee flexion. Changing the stiffness of the LCL only affected the

varus rotation of the knee. Decreasing the stiffness of the MCL changed laxity more than decreasing the stiffness of the LCL at both knee flexion angles. Changing the stiffness of the MCL only affected the valgus rotation of the knee.

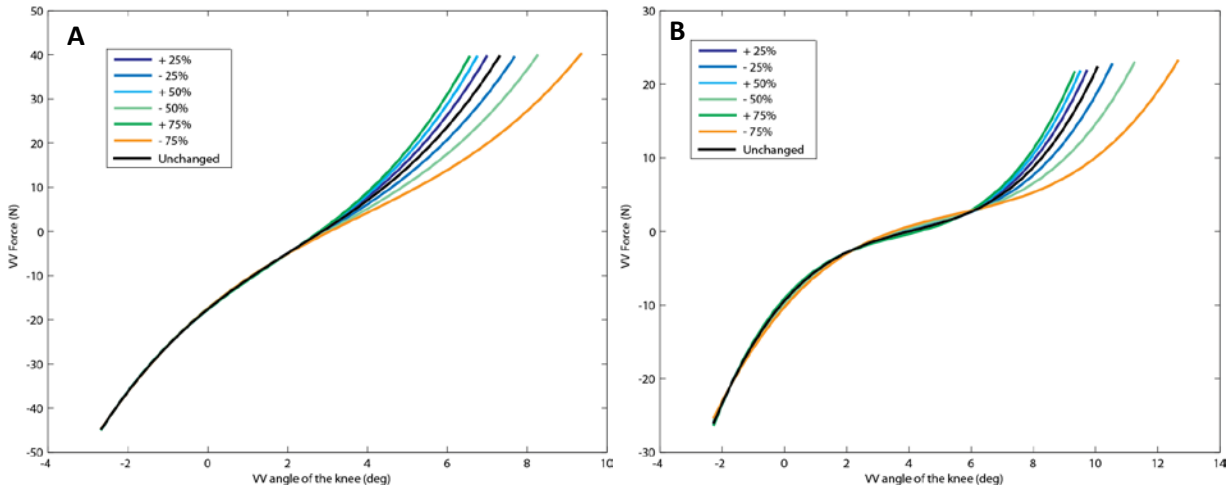

Figure 22: LCL ligament level stiffness simulations (A) 0° and (B) 20° knee flexion

Table 28: LCL ligament level stiffness simulations, 0° knee flexion

Simulation	Laxity (º)	Δ Laxity (º)	ΔVarus (º)	Δ Valgus (º)
Minus 75%	11.69	2.12	2.10	0.02
Minus 50%	10.56	0.99	0.98	0.01
Minus 25%	9.98	0.41	0.40	0.01
Unchanged	9.57	-	-	-
Plus 25%	9.24	0.34	0.33	0.00
Plus 50%	8.98	0.59	0.59	0.00
Plus 75%	8.77	0.80	0.79	0.01

Table 29: LCL ligament level stiffness simulations, 20° knee flexion

Simulation	Laxity (º)	Δ Laxity (º)	ΔVarus (º)	Δ Valgus (º)
Minus 75%	11.10	1.67	1.68	0.02
Minus 50%	10.18	0.76	0.75	0.00
Minus 25%	9.71	0.28	0.29	0.01
Unchanged	9.57	-	-	-
Plus 25%	9.23	0.20	0.20	0.00
Plus 50%	9.09	0.34	0.35	0.01
Plus 75%	8.97	0.46	0.46	0.00

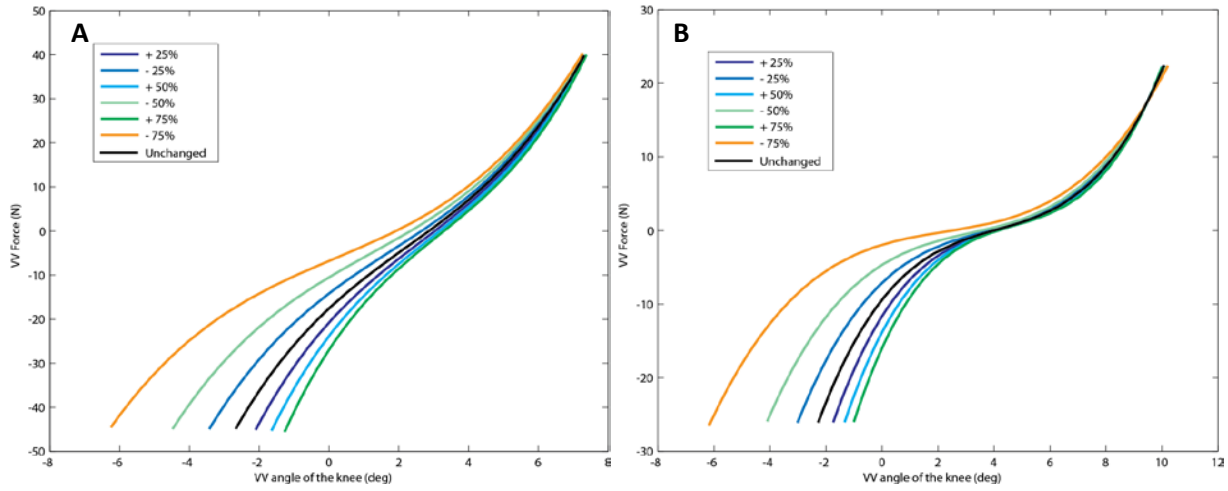

Figure 23: MCL ligament level stiffness simulations (A) 0° and (B) 20° knee flexion

Table 30: MCL ligament level stiffness simulations, 0° knee flexion

Simulation	Laxity (º)	Δ Laxity (º)	ΔVarus (º)	Δ Valgus (º)
Minus 75%	12.85	3.28	0.24	3.52
Minus 50%	11.20	1.63	0.13	1.76
Minus 25%	10.24	0.66	0.07	0.73
Unchanged	9.57	-	-	-
Plus 25%	9.06	0.51	0.05	0.56
Plus 50%	8.66	0.92	0.09	1.00
Plus 75%	8.32	1.26	0.11	1.37

Table 31: MCL ligament level stiffness simulations, 20° knee flexion

Simulation	Laxity (º)	Δ Laxity (º)	ΔVarus (º)	Δ Valgus (º)
Minus 75%	11.87	2.44	0.39	2.84
Minus 50%	10.63	1.21	0.13	1.34
Minus 25%	9.90	0.47	0.05	0.53
Unchanged	9.57	-	-	-
Plus 25%	9.08	0.35	0.03	0.38
Plus 50%	8.82	0.61	0.05	0.66
Plus 75%	8.61	0.82	0.07	0.89

c. Band level

Changing the stiffness of the anterior or posterior band of the LCL resulted in approximately equal changes in laxity at 0° and 20° knee flexion. Changing the stiffness of either band of the LCL only affected the varus rotation of the knee.

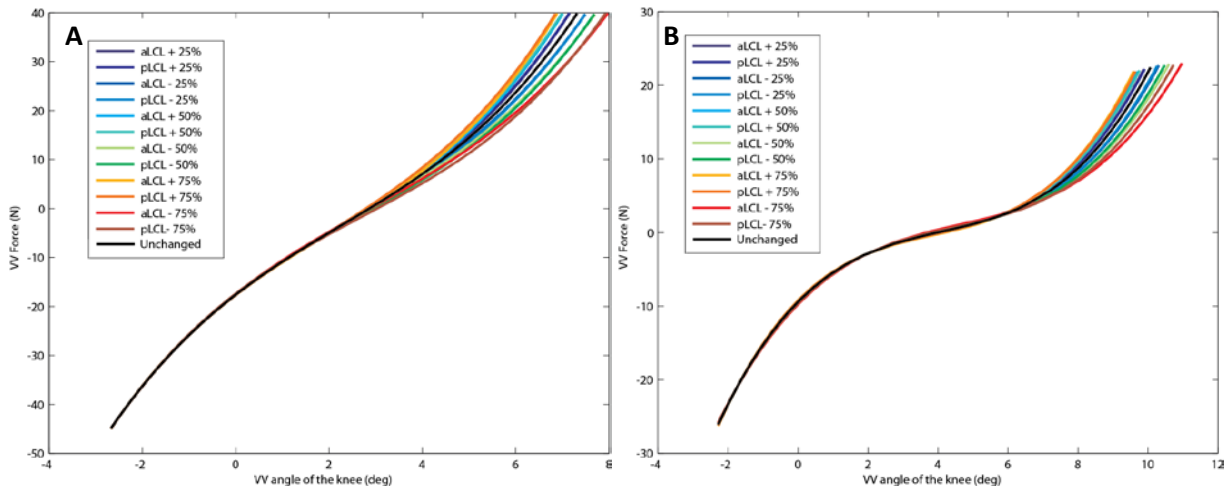

Figure 24: LCL band level stiffness simulations (A) 0° and (B) 20° knee flexion

Table 32: Anterior LCL band level stiffness simulations, 0° knee flexion

Simulation	Laxity (º)	Δ Laxity (º)	ΔVarus (º)	Δ Valgus (º)
Minus 75%	10.27	0.70	0.70	0.00
Minus 50%	10.00	0.42	0.42	0.00
Minus 25%	9.77	0.20	0.20	0.00
Unchanged	9.57	-	-	-
Plus 25%	9.39	0.18	0.18	0.00
Plus 50%	9.24	0.33	0.33	0.00
Plus 75%	9.11	0.46	0.46	0.00

Table 33: Anterior LCL band level stiffness simulations, 20° knee flexion

Simulation	Laxity (º)	Δ Laxity (º)	ΔVarus (º)	Δ Valgus (º)
Minus 75%	9.99	0.56	0.56	0.01
Minus 50%	9.75	0.32	0.32	0.00
Minus 25%	9.57	0.14	0.14	0.00
Unchanged	9.57	-	-	-
Plus 25%	9.33	0.10	0.10	0.00
Plus 50%	9.22	0.21	0.21	0.00
Plus 75%	9.14	0.29	0.29	0.00

Table 34: Posterior LCL band level stiffness simulations, 0° knee flexion

Simulation	Laxity (º)	Δ Laxity (º)	ΔVarus (º)	Δ Valgus (º)
Minus 75%	10.20	0.63	0.62	0.01
Minus 50%	9.96	0.39	0.38	0.01
Minus 25%	9.76	0.19	0.19	0.00
Unchanged	9.57	-	-	-
Plus 25%	9.39	0.18	0.18	0.00
Plus 50 %	9.23	0.34	0.34	0.00
Plus 75%	9.11	0.46	0.48	0.01

Table 35: Posterior LCL band level stiffness simulations, 20° knee flexion

Simulation	Laxity (º)	Δ Laxity (º)	ΔVarus (º)	Δ Valgus (º)
Minus 75%	9.86	0.43	0.43	0.01
Minus 50%	9.68	0.25	0.26	0.01
Minus 25%	9.54	0.12	0.12	0.00
Unchanged	9.57	-	-	-
Plus 25%	9.33	0.10	0.10	0.00
Plus 50%	9.24	0.19	0.19	0.01
Plus 75%	9.17	0.26	0.27	0.01

Changing the stiffness of the anterior band of the MCL changed laxity more than changing the stiffness of the posterior band of the MCL at 0° and 20° knee flexion.

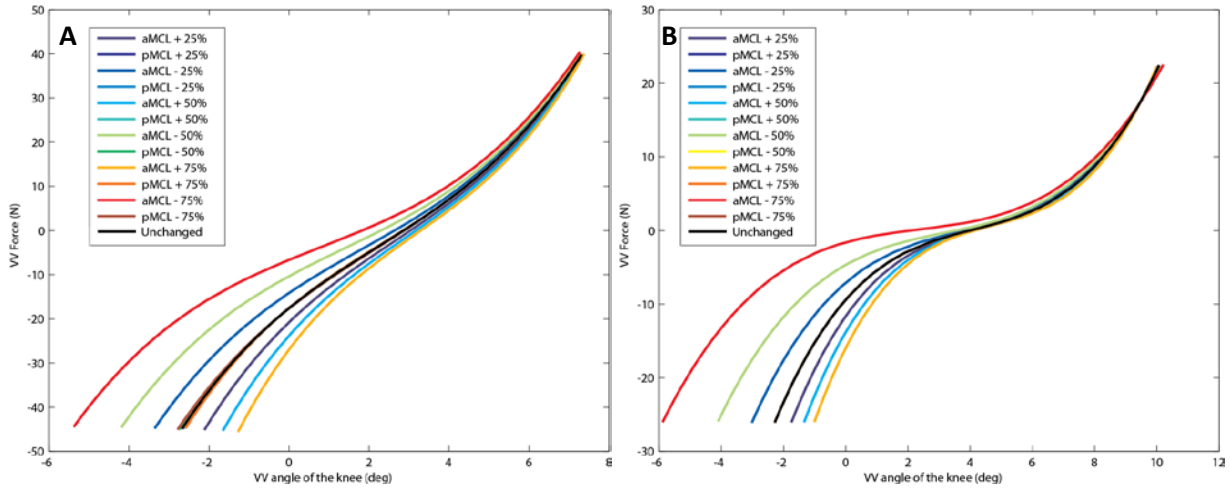

Figure 25: MCL band level stiffness simulations (A) 0° and (B) 20° knee flexion

Table 36: Anterior MCL band level stiffness simulations, 0° knee flexion

Simulation	Laxity (º)	Δ Laxity (º)	ΔVarus (º)	Δ Valgus (º)
Minus 75%	12.11	2.54	0.19	2.73
Minus 50%	10.97	1.40	0.13	1.53
Minus 25%	10.18	0.61	0.07	0.68
Unchanged	9.57	-	-	-
Plus 25%	9.07	0.50	0.05	0.55
Plus 50%	8.66	0.91	0.09	0.10
Plus 75%	8.32	1.26	0.11	1.37

Table 37: Anterior MCL band level stiffness simulations, 20° knee flexion

Simulation	Laxity (º)	Δ Laxity (º)	ΔVarus (º)	Δ Valgus (º)
Minus 75%	11.83	2.40	0.38	2.78
Minus 50%	9.43	0.00	0.00	0.00
Minus 25%	9.90	0.47	0.05	0.53
Unchanged	9.57	-	-	-
Plus 25%	9.08	0.35	0.03	0.38
Plus 50%	8.82	0.61	0.05	0.66
Plus 75%	8.61	0.82	0.07	0.89

Table 38: Posterior MCL band level stiffness simulations, 0° knee flexion

Simulation	Laxity (º)	Δ Laxity (º)	ΔVarus (º)	Δ Valgus (º)
Minus 75%	9.66	0.08	0.01	0.08
Minus 50%	9.63	0.05	0.00	0.05
Minus 25%	9.60	0.03	0.00	0.02
Unchanged	9.57	-	-	-
Plus 25%	9.55	0.02	0.00	0.02
Plus 50%	9.53	0.05	0.00	0.04
Plus 75%	9.50	0.07	0.01	0.06

Table 39: Posterior MCL band level stiffness simulations, 20° knee flexion

Simulation	Laxity (º)	Δ Laxity (º)	ΔVarus (º)	Δ Valgus (º)
Minus 75%	9.43	0.00	0.00	0.00
Minus 50%	9.43	0.00	0.00	0.00
Minus 25%	9.43	0.00	0.00	0.00
Unchanged	9.57	-	-	-
Plus 25%	9.43	0.00	0.00	0.00
Plus 50%	9.43	0.00	0.00	0.00
Plus 75%	9.43	0.00	0.00	0.00

4.1.3 Translated attachment sites

Translating the attachment sites of the LCL in the anterior-posterior or superior-inferior directions did not change joint laxity at 0° knee flexion. Translating the MCL in the superior direction decreased joint laxity at 0° knee flexion. For both the LCL and MCL, translating attachment sites at 20° knee flexion changed laxity more than translating attachment sites at 0° knee flexion.

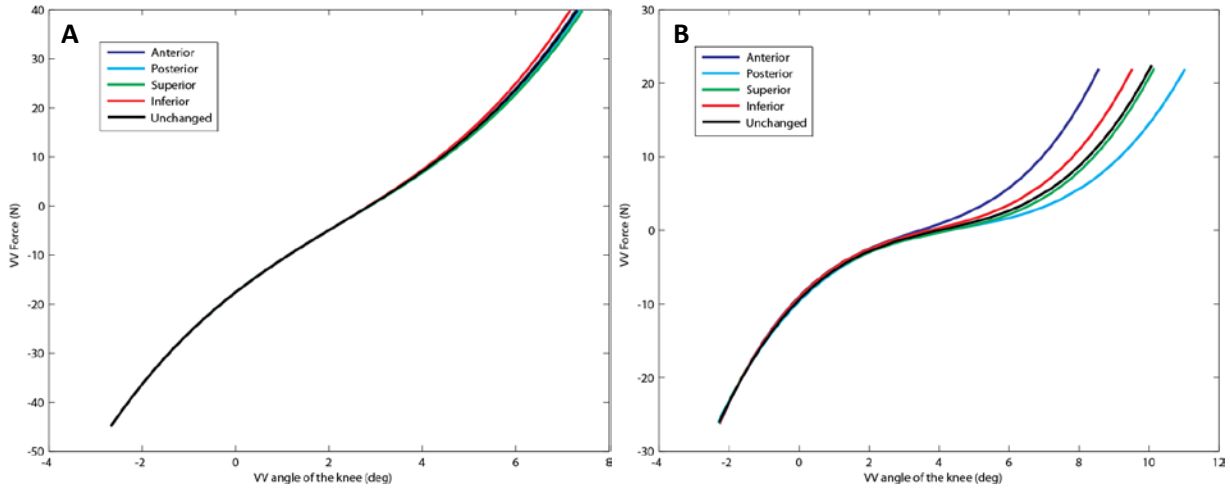

Figure 26: LCL attachment site simulations (A) 0° and (B) 20° knee flexion

Table 40: LCL attachment site simulations, 0° knee flexion

Simulation	Laxity (º)	Δ Laxity (º)	ΔVarus (º)	Δ Valgus (º)
Unchanged	9.57	-	-	-
Anterior	9.54	0.03	0.03	0.00
Posterior	9.62	0.05	0.05	0.00
Superior	9.70	0.13	0.12	0.00
Inferior	9.41	0.16	0.16	0.00

Table 41: LCL attachment site simulations, 20° knee flexion

Simulation	Laxity (º)	Δ Laxity (º)	ΔVarus (º)	Δ Valgus (º)
Unchanged	9.57	-	-	-
Anterior	8.23	1.20	1.32	0.12
Posterior	10.20	0.77	0.87	0.10
Superior	9.44	0.01	0.11	0.10
Inferior	9.08	0.35	0.43	0.09

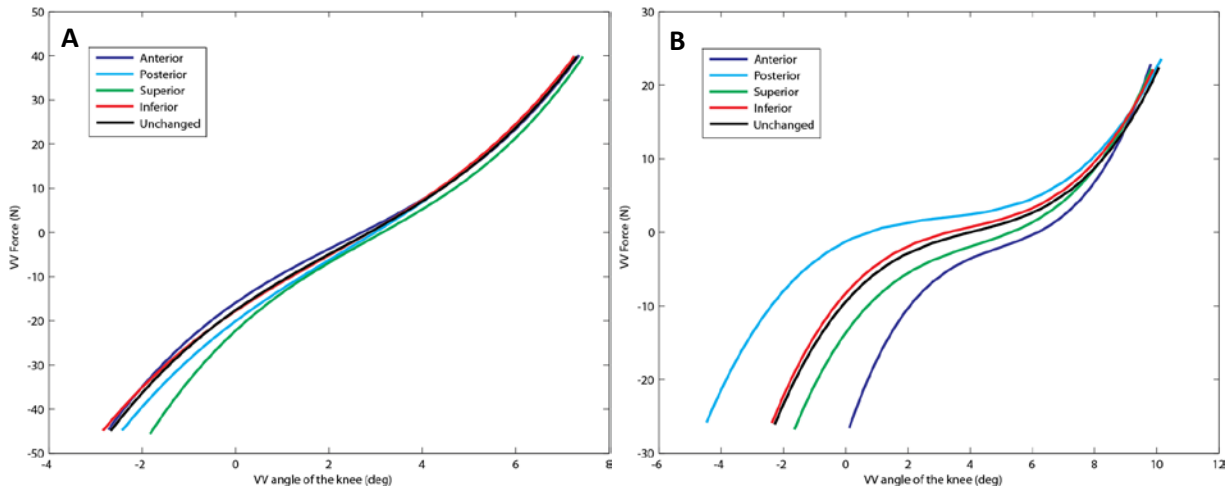

Figure 27: MCL attachment site simulations (A) 0° and (B) 20° knee flexion

Table 42: MCL attachment site simulations, 0° knee flexion

Simulation	Laxity (º)	Δ Laxity (º)	ΔVarus (º)	Δ Valgus (º)
Unchanged	9.57	-	-	-
Anterior	9.70	0.13	0.02	0.11
Posterior	9.30	0.27	0.00	0.27
Superior	8.91	0.67	0.16	0.83
Inferior	9.64	0.07	0.05	0.13

Table 43: MCL attachment site simulations, 20° knee flexion

Simulation	Laxity (º)	Δ Laxity (º)	ΔVarus (º)	Δ Valgus (º)
Unchanged	9.57	-	-	-
Anterior	7.45	1.98	0.24	2.21
Posterior	10.83	1.40	0.68	2.08
Superior	8.58	0.84	0.02	0.87
Inferior	9.39	0.04	0.25	0.21

4.1.4 "X" Configuration

Creating an X configuration with the bands of the LCL did not affect joint laxity. Switching the femoral attachment sites of the MCL increased varus and valgus rotation while switching the tibial attachment sites of the MCL caused the simulation to fail. This analysis was not performed at 20° knee flexion.

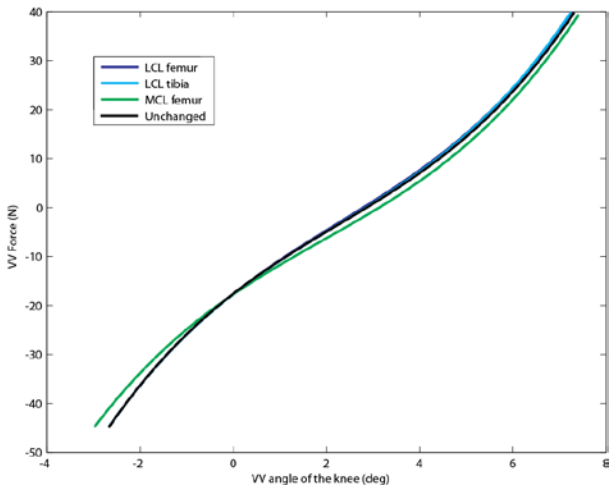

Figure 28: X configuration simulations, 0º knee flexion

Table 44: X configuration simulations, 0º knee flexion

Simulation	Laxity (º)	Δ Laxity (º)	ΔVarus (º)	Δ Valgus (º)
Unchanged	9.57	-	-	-
LCL femur	9.55	9.55	0.02	0.00
LCL tibia	9.50	9.50	0.07	0.00
MCL femur	9.91	0.08	0.08	0.26

.1.5 Adding bands

Adding bands (either more anteriorly or more posteriorly) to the LCL did not affect joint laxity. Adding more anterior bands increased valgus rotation while adding more posterior bands to the MCL decreased valgus rotation at 0° knee flexion. Adding more anterior or more posterior bands to the MCL at 20° knee flexion increased valgus rotation.

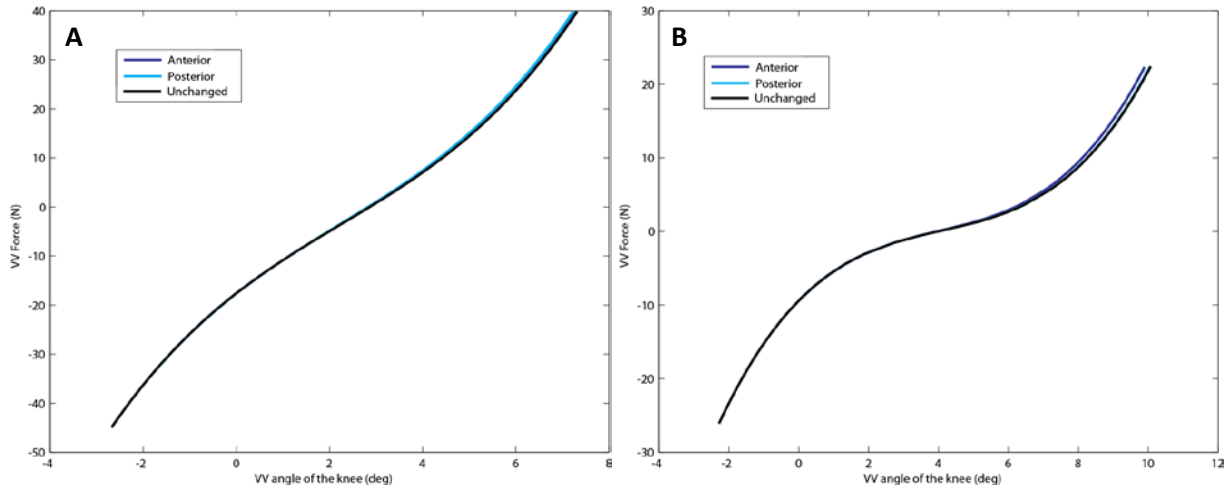

Figure 29: Adding LCL bands, (A) 0° and (B) 20° knee flexion

Table 45: Adding LCL bands, 0° knee flexion

Simulation	Laxity (º)	Δ Laxity (º)	ΔVarus (º)	Δ Valgus (º)
Unchanged	9.57	-	-	-
Anterior	9.54	0.03	0.03	0.00
Posterior	9.49	0.08	0.08	0.00

Table 46: Adding LCL bands, 20° knee flexion

Simulation	Laxity (º)	Δ Laxity (º)	ΔVarus (º)	Δ Valgus (º)
Unchanged	9.57	-	-	-
Anterior	9.31	0.27	0.14	0.02
Posterior	9.42	0.15	0.01	0.00

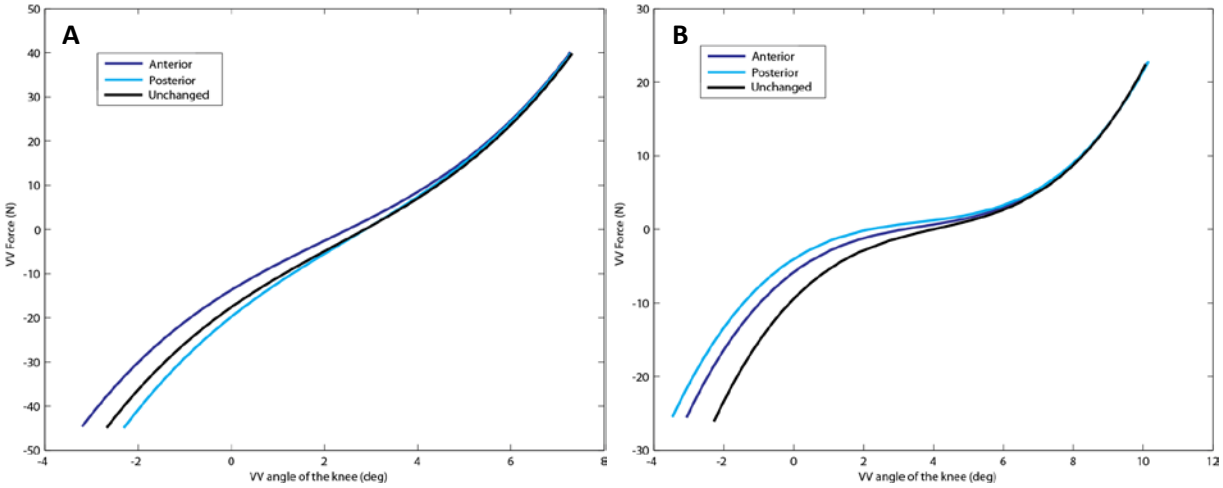

Figure 30: Adding MCL bands (A) 0° and (B) 20° knee flexion

Table 47: Adding MCL bands, 0° knee flexion

Simulation	Laxity (º)	Δ Laxity (º)	ΔVarus (º)	Δ Valgus (º)
Unchanged	9.57	-	-	-
Anterior	10.07	0.4950	0.0677	0.5626
Posterior	9.21	0.3635	0.0071	0.3705

Table 48: Adding MCL bands, 20° knee flexion

Simulation	Laxity (º)	Δ Laxity (º)	ΔVarus (º)	Δ Valgus (º)
Unchanged	9.57	-	-	-
Anterior	10.10	0.53	0.09	0.76
Posterior	10.39	0.82	0.21	1.18

4.2 Four Band Model Sensitivity

The baseline simulation for the four band model depended on the location of the additional bands and therefore listed under each section.

4.2.1 Anterior MCL fans

For all variations to the anteriorly added fans, the baseline simulation was the four band model with anteriorly added bands and unchanged configuration of the bands (all bands were approximately parallel in the sagittal plane) (Figure 9, A). A more anterior fan, seen as a "V" from the point of view of the tibia, of the two most anterior bands increased valgus rotation at 0° and 20° knee flexion. Band configuration of the two most posterior bands did not influence joint laxity at either flexion angle. A more anterior fan, seen as a "V from the point of view of the femur, of the two most anterior bands decreased valgus rotation at 20° knee flexion.

a. Tibial fans

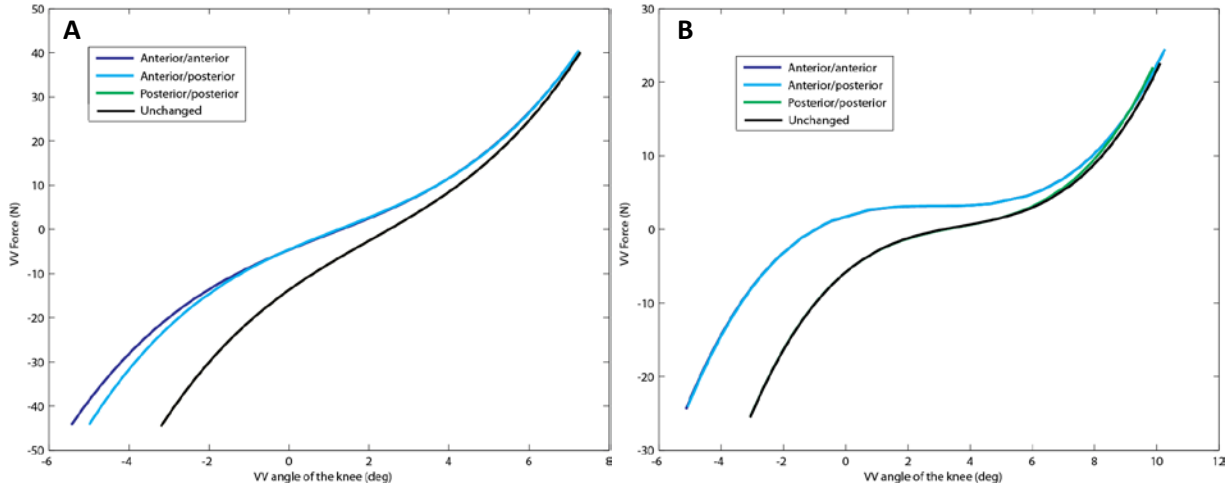

Figure 31: Anterior MCL tibial fans (A) 0° and (B) 20° knee flexion

Table 49: Anterior MCL tibial fans, 0° knee flexion

Simulation	Laxity (º)	Δ Laxity (º)	ΔVarus (º)	Δ Valgus (º)
Anterior/anterior	12.24	2.17	0.12	2.28
Anterior/posterior	11.85	1.78	0.08	1.87
Posterior/posterior	10.07	0.00	0.00	0.00

Table 50: Anterior MCL tibial fans, 20° knee flexion

Simulation	Laxity (º)	Δ Laxity (º)	ΔVarus (º)	Δ Valgus (º)
Anterior/anterior	11.14	1.07	1.07	2.10
Anterior/posterior	11.13	1.06	1.06	2.09
Posterior/posterior	9.92	0.14	0.16	0.02

b. Femoral fans

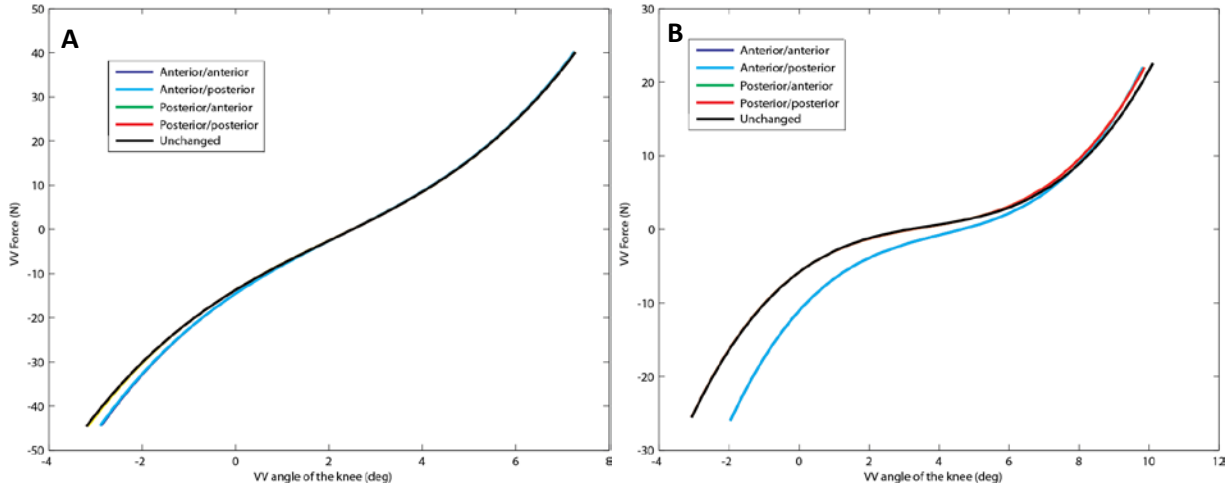

Figure 32: Anterior MCL femoral fans (A) 0° and (B) 20° knee flexion

Table 51: Anterior MCL femoral fans, 0° knee flexion

Simulation	Laxity (º)	Δ Laxity (º)	ΔVarus (º)	Δ Valgus (º)
Anterior/anterior	9.77	0.29	0.01	0.29
Anterior/posterior	9.79	0.27	0.01	0.27
Posterior/anterior	10.04	0.03	0.00	0.03
Posterior/posterior	10.07	0.00	0.00	0.00

Table 52: Anterior MCL femoral fans, 20° knee flexion

Simulation	Laxity (º)	Δ Laxity (º)	ΔVarus (º)	Δ Valgus (º)
Anterior/anterior	9.01	1.05	0.03	1.12
Anterior/posterior	9.01	1.05	0.03	1.12
Posterior/anterior	9.92	0.14	0.16	0.02
Posterior/posterior	9.92	0.14	0.16	0.02

c. Anterior fans

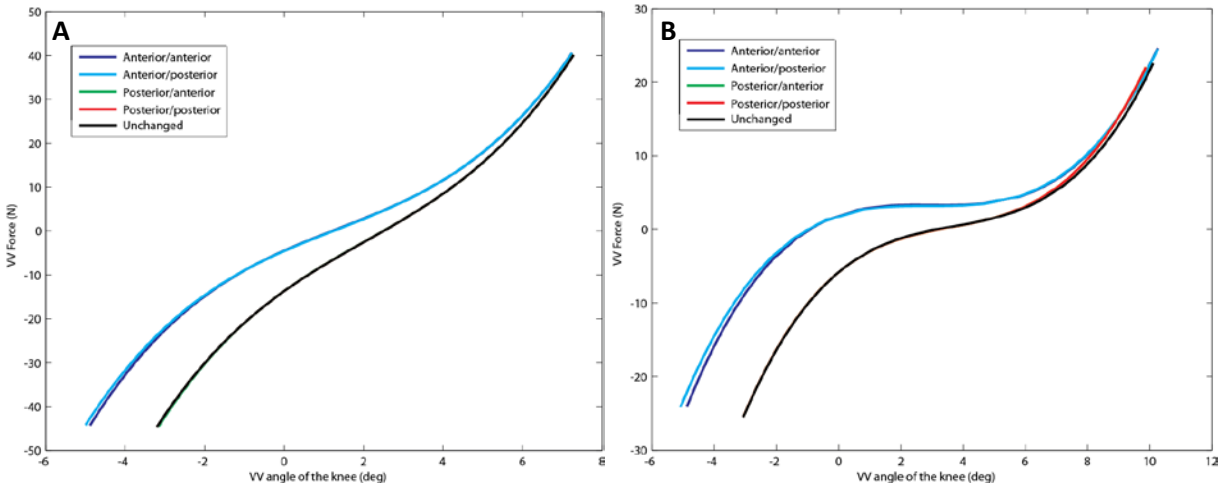

Figure 33: Anterior MCL anterior fans (A) 0° and (B) 20° knee flexion

Table 53: Anterior MCL anterior fans, 0° knee flexion

Simulation	Laxity (º)	Δ Laxity (º)	ΔVarus (º)	Δ Valgus (º)
Anterior/anterior	11.75	1.68	0.08	1.76
Anterior/posterior	11.85	1.78	0.08	1.87
Posterior/anterior	10.04	0.03	0.00	0.03
Posterior/posterior	10.07	0.00	0.00	0.00

Table 54: Anterior MCL anterior fans, 20° knee flexion

Simulation	Laxity (º)	Δ Laxity (º)	ΔVarus (º)	Δ Valgus (º)
Anterior/anterior	11.02	0.95	1.06	1.98
Anterior/posterior	11.13	1.06	1.06	2.09
Posterior/anterior	9.92	0.14	0.16	0.02
Posterior/posterior	9.92	0.14	0.16	0.02

d. Posterior fans

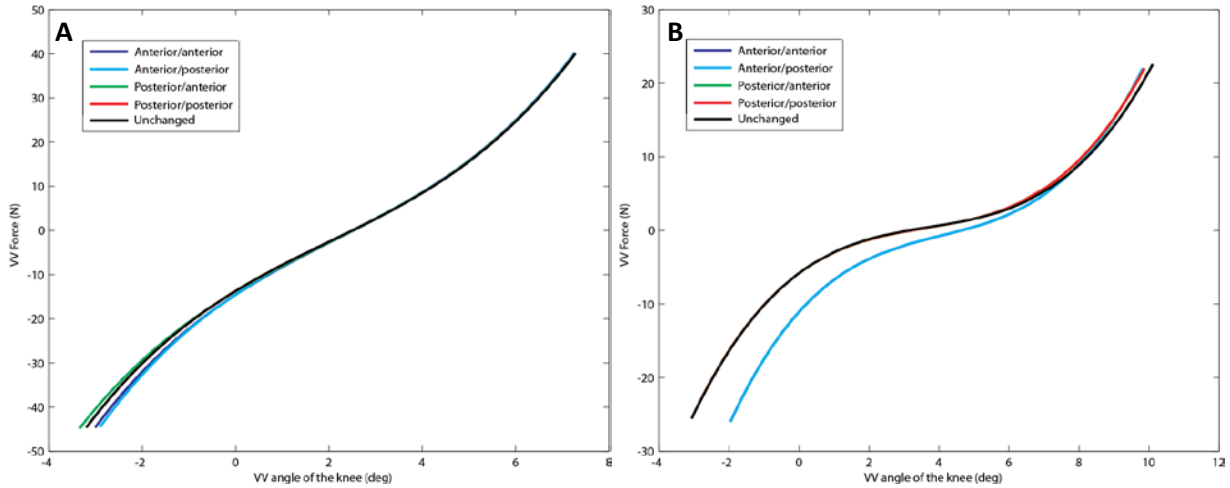

Figure 34: Anterior MCL posterior V fans (A) 0° and (B) 20° knee flexion

Table 55: Anterior MCL posterior fans, 0° knee flexion

Simulation	Laxity (º)	Δ Laxity (º)	ΔVarus (º)	Δ Valgus (º)
Anterior/anterior	9.88	0.19	0.00	0.19
Anterior/posterior	9.79	0.27	0.01	0.27
Posterior/anterior	10.18	0.11	0.00	0.11
Posterior/posterior	10.07	0.00	0.00	0.00

Table 56: Anterior MCL posterior fans, 20° knee flexion

Simulation	Laxity (º)	Δ Laxity (º)	ΔVarus (º)	Δ Valgus (º)
Anterior/anterior	9.01	1.05	0.03	1.12
Anterior/posterior	9.01	1.05	0.03	1.12
Posterior/anterior	9.92	0.14	0.16	0.02
Posterior/posterior	9.92	0.14	0.16	0.02

4.2.2 Posterior MCL bands

For all variations to the posteriorly added fans, the baseline simulation was the four band model with posteriorly added bands and unchanged configuration of the bands (all bands were approximately parallel in the sagittal plane) (Figure 9, B). A more posterior fan, seen as a "V" from the point of view of the tibia, of the two most anterior bands decreased valgus rotation at 0° and 20° knee flexion and affected both varus and valgus rotations. A more

posterior fan, seen as a “V” from the point of view of the femur, of the two most anterior bands increased valgus rotation at 20° knee flexion.

a. Tibial fans

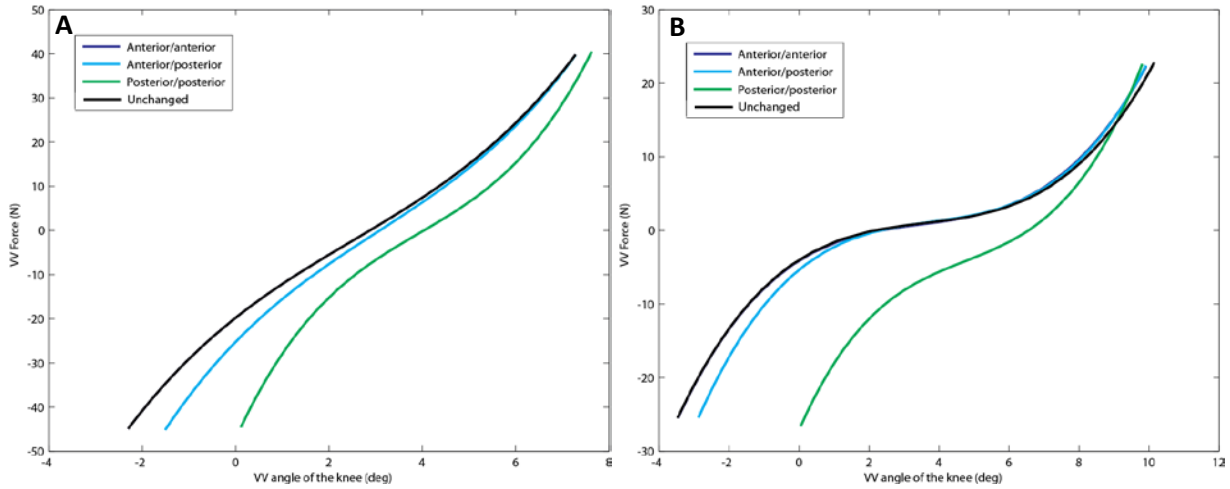

Figure 35: Posterior MCL tibial fans (A) 0° and (B) 20° knee flexion

Table 57: Posterior MCL tibial fans, 0° knee flexion

Simulation	Laxity (º)	Δ Laxity (º)	ΔVarus (º)	Δ Valgus (º)
Anterior/anterior	9.21	0.00	0.00	0.00
Anterior/posterior	8.48	0.73	0.04	0.77
Posterior/posterior	7.24	1.97	0.28	2.25

Table 58: Posterior MCL tibial fans, 20° knee flexion

Simulation	Laxity (º)	Δ Laxity (º)	ΔVarus (º)	Δ Valgus (º)
Anterior/anterior	10.22	1.01	0.14	0.03
Anterior/posterior	9.86	0.65	0.12	0.42
Posterior/posterior	7.12	2.09	0.48	3.75

b. Femoral fans

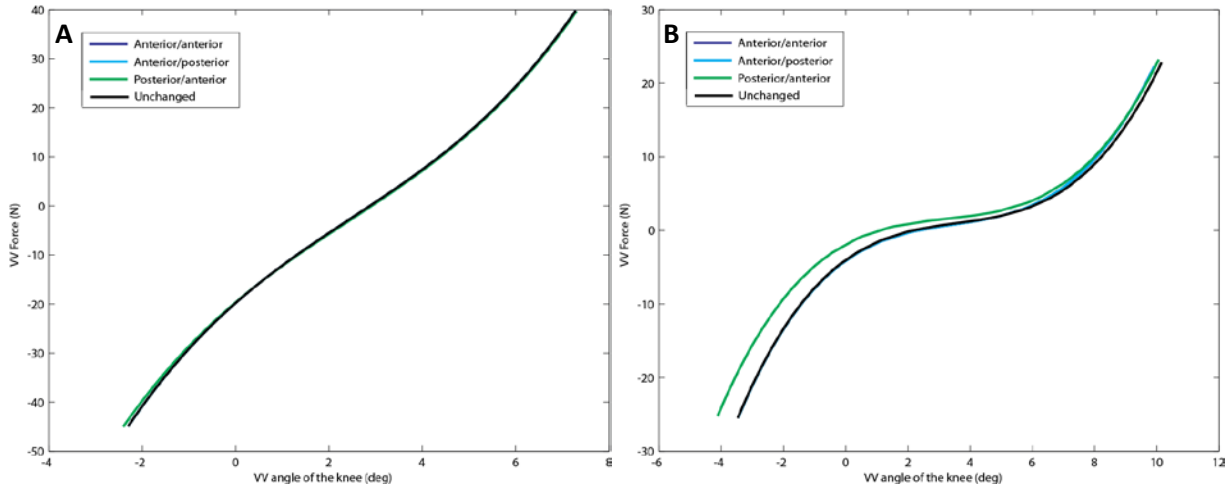

Figure 36: Posterior MCL femoral fans (A) 0° and (B) 20° knee flexion

Table 59: Posterior MCL femoral fans, 0° knee flexion

Simulation	Laxity (º)	Δ Laxity (º)	ΔVarus (º)	Δ Valgus (º)
Anterior/anterior	9.21	0.00	0.00	0.00
Anterior/posterior	9.21	0.00	0.00	0.00
Posterior/anterior	9.31	0.10	0.02	0.08

Table 60: Posterior MCL femoral fans, 20° knee flexion

Simulation	Laxity (º)	Δ Laxity (º)	ΔVarus (º)	Δ Valgus (º)
Anterior/anterior	10.22	1.01	0.14	0.03
Anterior/posterior	10.22	1.01	0.14	0.03
Posterior/anterior	10.63	1.42	0.37	0.60

c. Anterior fans

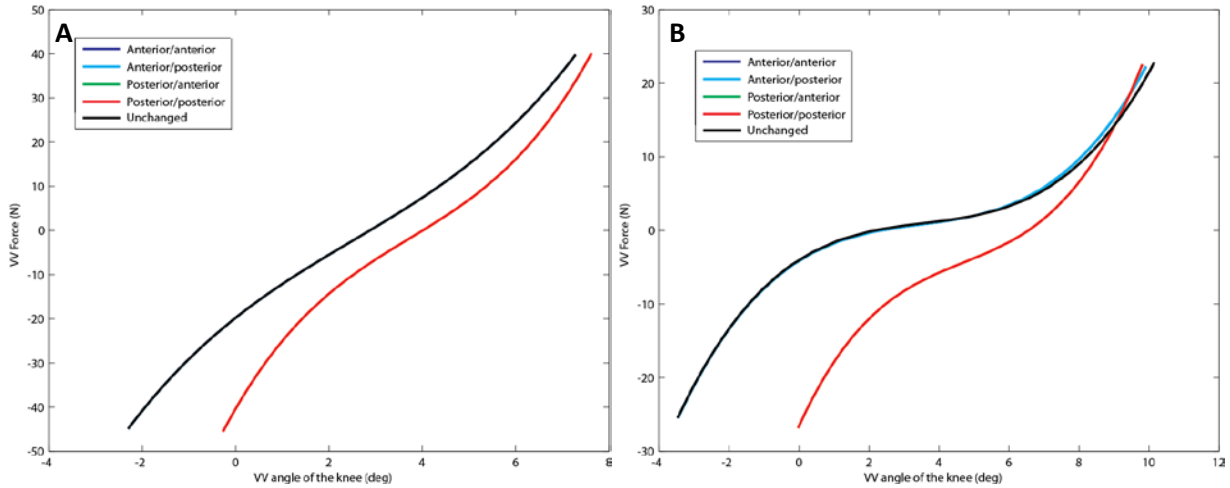

Figure 37: Posterior MCL anterior fans (A) 0° and (B) 20° knee flexion

Table 61: Posterior MCL anterior fans, 0° knee flexion

Simulation	Laxity (º)	Δ Laxity (º)	ΔVarus (º)	Δ Valgus (º)
Anterior/anterior	9.21	0.00	0.00	0.00
Anterior/posterior	9.21	0.00	0.00	0.00
Posterior/anterior	7.55	1.66	0.30	1.95
Posterior/posterior	7.55	1.66	0.30	1.95

Table 62: Posterior MCL anterior fans, 20° knee flexion

Simulation	Laxity (º)	Δ Laxity (º)	ΔVarus (º)	Δ Valgus (º)
Anterior/anterior	10.22	1.01	0.14	0.03
Anterior/posterior	10.22	1.01	0.14	0.03
Posterior/anterior	7.12	2.09	0.48	3.75
Posterior/posterior	7.12	2.09	0.48	3.75

d. Posterior fans

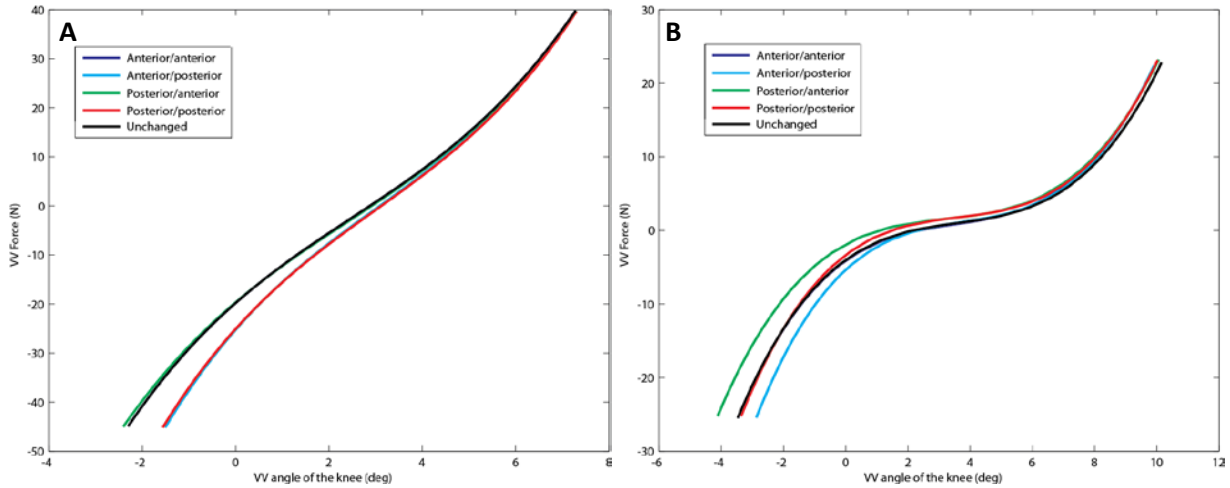

Figure 38: Posterior MCL posterior fans (A) 0° and (B) 20° knee flexion

Table 63: Posterior MCL posterior fans, 0° knee flexion

Simulation	Laxity (º)	Δ Laxity (º)	ΔVarus (º)	Δ Valgus (º)
Anterior/anterior	9.21	0.00	0.00	0.00
Anterior/posterior	8.48	0.73	0.04	0.77
Posterior/anterior	9.31	0.10	0.02	0.08
Posterior/posterior	8.54	0.67	0.06	0.72

Table 64: Posterior MCL posterior fans, 20° knee flexion

Simulation	Laxity (º)	Δ Laxity (º)	ΔVarus (º)	Δ Valgus (º)
Anterior/anterior	10.22	1.01	0.14	0.03
Anterior/posterior	9.86	0.65	0.12	0.42
Posterior/anterior	10.63	1.42	0.37	0.60
Posterior/posterior	10.19	0.98	0.28	0.07

4.3 Discussion

In this study, specimen-specific simulations of TKA motion showed clear differences in the varus-valgus behavior of the knee with varying ligament modeling choices. These results suggest that ligament slack length has the greatest impact on varus-valgus laxity and should receive special attention in any ligament modeling effort. Ligament stiffness only affected joint laxity when altered by 50% of the optimized value and was not considered critical to varus-valgus laxity in this model. Increasing the number bands of the MCL affected the laxity and indicated sensitivity to the anterior-posterior location of the additional bands. However, increasing the number of bands of the LCL did not affect joint laxity. The LCL and MCL were found to engage differently, demonstrating differences in their contributions to varus-valgus rotation in this model.

While changes in ligament slack length affected varus-valgus laxity more than changes in ligament stiffness in this study, the original (not optimized) values for ligament properties were adapted from a previous study [15, 69]. It is not known whether a different set of original values would yield the same optimized ligament properties. The results at 0° knee flexion were the primary consideration of this study because the collateral ligaments are known to be fully engaged at full extension. However, results at 20° knee flexion may be considered more clinically relevant for insight of the contribution of ligament properties during the weight-acceptance phase of walking.

These results suggest the MCL is more sensitive to changes in the number and location of bands than the LCL. Anatomically, the MCL is longer and wider than the LCL and the two band model may not be sufficient to accurately replicate the dynamics of the MCL. The MCL

may require more complex modeling efforts (e.g., more bands or altered band configuration) to represent the complex ligament structure.

These results provide some insight of the sensitivity of ligament modeling choices but there are limitations to this study. The analysis conducted only included one specimen and contributions of implant or wrapping surface geometries were not considered. As well, only one modeling parameter was altered at a time and only varus-valgus rotation was considered. Altering more than one parameter may redefine which combinations of modeling choices will most influence knee kinematics.

Understanding the sensitivity of ligament modeling choices informs the creation of computer simulations of TKA motions that can provide reliable insight of how surgical technique influences knee function. By understanding how ligament modeling choices impact knee motion, researchers can more easily create more biofidelic and patient-specific simulations to predict postoperative function based on surgical technique.

Chapter 5: Conclusion

5.1 Contributions

Total knee arthroplasty is a common end of stage treatment for osteoarthritis of the knee. However, TKA does not always produce optimal functional results. Simulations of TKA can help researchers understand how intraoperative decisions will affect the patient after surgery. The structures surrounding the knee are complex and there are no agreed upon method for how ligaments should be modeled. Previous simulation studies have not investigated the sensitivity of models to incremental changes in ligament properties. A model and forward dynamic computer simulation of varus-valgus motion were used to investigate the kinematic

effect of altering collateral ligament stiffness, slack length, attachment site, and number and arrangement of bands. Changes in ligament slack length and additional bands representing the MCL had the most effect on the varus-valgus laxity of the joint. The results from this study were used to improve a TKA model as an integral part of developing an optimization technique to determine patient-specific ligament properties (developed by Joseph Ewing, NMBL).

5.2 Additional Applications

This research determined the effects of varying ligament modeling choices on varus-valgus rotation. Additional applications of this work may include a parametric analysis of applied internal-external or anterior-posterior motions and motions at deeper knee flexion angles. Another study may alter two modeling choices simultaneously (e.g., slack length sensitivity of the four band model). This type of analysis is currently being used to determine the sensitivity of ligament modeling choices of the anterior and posterior cruciate ligaments to create a model of the natural knee.

5.3 Future Work

Using the findings of this research and other parametric analyses, a patient-specific model of TKA can be integrated into simulations of normal patient activities. Simulations of walking and squatting motions include muscles and can simulate muscle weakness from disease. The combination of models can provide insight of how component alignment and ligament balancing during surgery translate to normal patient activities. By developing patient-specific and biofidelic models of TKA in simulations of daily activities, researchers can work towards predicting functional outcomes as a result of surgical technique and move towards improving patient outcomes following surgery.

5.4 Summary

A sensitivity study of collateral ligament modeling choices was done using a lumped sum model of TKA in a forward dynamic, varus-valgus simulation [15, 69]. Slack length, stiffness, attachment site, and the number and arrangement of bands were investigated in this study. Ligament slack length and the number of bands of the MCL were the most sensitive to modeling choices. Understanding the sensitivity of ligament modeling choices is an important step in developing a more accurate model of TKA to study the effect of intraoperative decisions on knee kinematics and predict post-operative patient function.

References

1. Hootman, J.M., C.G. Helmick, *Projections of US Prevalence of Arthritis and Associated Activity Limitations.* Arthritis & Rheumatism, 2006. **54**(1): p. 226-9.
2. *Osteoarthritis*. 2009 [cited 2013 16 May]; Available from: http://www.cdc.gov/arthritis/basics/osteoarthritis.htm.
3. Kurtz, S., K. Ong, E. Lau, F. Mowat, M. Halpern, *Projections of primary and revision hip and knee arthroplasty in the United States from 2005 to 2030.* J Bone Joint Surg Am., 2007. **89**(4): p. 780-5.
4. Jiang, C.C., J.N. Insall, *Effect of rotation on the axial alignment of the femur. Pitfalls of the use of femoral intramedullary guides in total knee arthroplasty.* Clin. Orthop Relat res, 1989(248): p. 50-6.
5. Meier, W., R. Mizner, R. Marcus, L. Dibble, C. Peters, P. Lastayo, *Total Knee Arthroplasty: Muscle Impairments, Functional Limitations, and Recommended Rehabilitation Approaches.* J Orthop Sports Phys Ther, 2008. **38**(5): p. 246-56.
6. Weiss, J.M., P.C. Noble, M.A. Conditt, H.W. Kohl, S. Roberts, K.F. Cook, M.J. Gordon, K.B. Mathis, *What functional activities are important to patients with knee replacements?* Clin Orthop Relat Res,, 2002. **404**: p. 172-88.
7. Byrne, J.M., W.H. Gage, S.D. Prentice, *Bilateral lower limb strategies used during a step-up task in individuals who have undergone unilateral total knee arthroplasty. .* Clin Biomech 2002. **17**(8): p. 580-5.
8. Mandeville, D., L.R. Osternig, L. Chou, *The effect of total knee replacement on dynamic support of the body during walking and stair ascent.* Clin Biomech, 2006. **22**(787-94).
9. Stulberg, S.D., P. Loan, and V. Sarin, *Computer-assisted navigation in total knee replacement: results of an initial experience in thirty-five patients.* J Bone Joint Surg Am, 2002. **84-A Suppl 2**: p. 90-8.
10. Fitzpatrick, C.K., C.W. Clary, and P.J. Rullkoetter, *The role of patient, surgical, and implant design variation in total knee replacement performance.* J Biomech, 2012. **45**(12): p. 2092-102.
11. Takahashi, T., Y. Wada, and H. Yamamoto, *Soft-tissue balancing with pressure distribution during total knee arthroplasty.* J Bone Joint Surg Br, 1997. **79**(2): p. 235-9.
12. Griffin, F.M., J.N. Insall, and G.R. Scuderi, *Accuracy of soft tissue balancing in total knee arthroplasty.* J Arthroplasty, 2000. **15**(8): p. 970-3.
13. Siston, R.A., et al., *Design and cadaveric validation of a novel device to quantify knee stability during total knee arthroplasty.* J Biomech Eng, 2012. **134**(11): p. 115001.
14. Delp, S.L., et al., *OpenSim: open-source software to create and analyze dynamic simulations of movement.* IEEE Trans Biomed Eng, 2007. **54**(11): p. 1940-50.
15. Piazza, S.J. and S.L. Delp, *Three-dimensional dynamic simulation of total knee replacement motion during a step-up task.* J Biomech Eng, 2001. **123**(6): p. 599-606.
16. Baldwin, M.A., et al., *Dynamic finite element knee simulation for evaluation of knee replacement mechanics.* J Biomech, 2012. **45**(3): p. 474-83.
17. Thompson, J.A., et al., *Biomechanical effects of total knee arthroplasty component malrotation: a computational simulation.* J Orthop Res, 2011. **29**(7): p. 969-75.
18. Nesline, M., *Biomechanics of a Posterior Substituting Knee During a Simulated Squatting Motion*, in *Department of Mechanical and Aerospace Engineering*2012, The Ohio State University: Columbus, Ohio. p. 57.
19. Piazza, S.J., et al., *Posterior tilting of the tibial component decreases femoral rollback in posterior-substituting knee replacement: a computer simulation study.* J Orthop Res, 1998. **16**(2): p. 264-70.

20. Trent, P.S., P.S. Walker, and B. Wolf, *Ligament length patterns, strength, and rotational axes of the knee joint.* Clin Orthop Relat Res, 1976(117): p. 263-70.
21. Brantigan, O.C., A.F. Voshell, *The Mechanics of the Ligaments and Menisci of the Knee Joint.* J Bone Joint Surg, 1941. **23**(1): p. 44-66.
22. Edwards, R.G., J.F. Lafferty, K.O. Lange, *Ligament Strain in the Human Knee Joint.* Journal of Basic Engineering (ASME), 1970: p. 131-6.
23. Markolf, K.L., J.S. Mensch, and H.C. Amstutz, *Stiffness and laxity of the knee--the contributions of the supporting structures. A quantitative in vitro study.* J Bone Joint Surg Am, 1976. **58**(5): p. 583-94.
24. Hsieh, H.H. and P.S. Walker, *Stabilizing mechanisms of the loaded and unloaded knee joint.* J Bone Joint Surg Am, 1976. **58**(1): p. 87-93.
25. Grood, E.S., et al., *Ligamentous and capsular restraints preventing straight medial and lateral laxity in intact human cadaver knees.* J Bone Joint Surg Am, 1981. **63**(8): p. 1257-69.
26. Quapp, K.M. and J.A. Weiss, *Material characterization of human medial collateral ligament.* J Biomech Eng, 1998. **120**(6): p. 757-63.
27. Robinson, J.R., A.M. Bull, and A.A. Amis, *Structural properties of the medial collateral ligament complex of the human knee.* J Biomech, 2005. **38**(5): p. 1067-74.
28. Blankevoort, L., R. Huiskes, and A. de Lange, *Recruitment of knee joint ligaments.* J Biomech Eng, 1991. **113**(1): p. 94-103.
29. Wijdicks, C.A., et al., *Structural properties of the primary medial knee ligaments.* Am J Sports Med, 2010. **38**(8): p. 1638-46.
30. Butler, D.L., M. D. Kay, D. C. Stouffer, *Comparison of Material Properties in Fascicle-Bone Untis from Human Patellar Tendon and Knee Ligaments.* J Biomechics 1986. **19**(6): p. 425-32.
31. Blankevoort, L. and R. Huiskes, *Ligament-bone interaction in a three-dimensional model of the knee.* J Biomech Eng, 1991. **113**(3): p. 263-9.
32. Bloemker, K.H., et al., *Computational knee ligament modeling using experimentally determined zero-load lengths.* Open Biomed Eng J, 2012. **6**: p. 33-41.
33. Shelburne, K.B., et al., *Effect of posterior tibial slope on knee biomechanics during functional activity.* J Orthop Res, 2011. **29**(2): p. 223-31.
34. Griffith, C.J., et al., *Force measurements on the posterior oblique ligament and superficial medial collateral ligament proximal and distal divisions to applied loads.* Am J Sports Med, 2009. **37**(1): p. 140-8.
35. Crowninshield, R., M.H. Pope, and R.J. Johnson, *An analytical model of the knee.* J Biomech, 1976. **9**(6): p. 397-405.
36. Wismans, J., et al., *A three-dimensional mathematical model of the knee-joint.* J Biomech, 1980. **13**(8): p. 677-85.
37. Moeinzadeh, M.H., A.E. Engin, and N. Akkas, *Two-dimensional dynamic modelling of human knee joint.* J Biomech, 1983. **16**(4): p. 253-64.
38. Blankevoort, L., et al., *Articular contact in a three-dimensional model of the knee.* J Biomech, 1991. **24**(11): p. 1019-31.
39. Blankevoort, L. and R. Huiskes, *Validation of a three-dimensional model of the knee.* J Biomech, 1996. **29**(7): p. 955-61.
40. Mommersteeg, T.J., et al., *A global verification study of a quasi-static knee model with multi-bundle ligaments.* J Biomech, 1996. **29**(12): p. 1659-64.
41. Mommersteeg, T.J., et al., *An inverse dynamics modeling approach to determine the restraining function of human knee ligament bundles.* J Biomech, 1997. **30**(2): p. 139-46.
42. Shelburne, K.B. and M.G. Pandy, *A musculoskeletal model of the knee for evaluating ligament forces during isometric contractions.* J Biomech, 1997. **30**(2): p. 163-76.

43. Li, G., et al., *A validated three-dimensional computational model of a human knee joint.* J Biomech Eng, 1999. **121**(6): p. 657-62.
44. Abdel-Rahman, E.M. and M.S. Hefzy, *Three-dimensional dynamic behaviour of the human knee joint under impact loading.* Med Eng Phys, 1998. **20**(4): p. 276-90.
45. Bei, Y. and B.J. Fregly, *Multibody dynamic simulation of knee contact mechanics.* Med Eng Phys, 2004. **26**(9): p. 777-89.
46. Amiri, S., et al., *Mechanics of the passive knee joint. Part 2: interaction between the ligaments and the articular surfaces in guiding the joint motion.* Proc Inst Mech Eng H, 2007. **221**(8): p. 821-32.
47. Guess, T.M., et al., *A subject specific multibody model of the knee with menisci.* Med Eng Phys, 2010. **32**(5): p. 505-15.
48. Essinger, J.R., et al., *A mathematical model for the evaluation of the behaviour during flexion of condylar-type knee prostheses.* J Biomech, 1989. **22**(11-12): p. 1229-41.
49. Garg, A. and P.S. Walker, *Prediction of total knee motion using a three-dimensional computer-graphics model.* J Biomech, 1990. **23**(1): p. 45-58.
50. Sathasivam, S. and P.S. Walker, *A computer model with surface friction for the prediction of total knee kinematics.* J Biomech, 1997. **30**(2): p. 177-84.
51. Martelli, S., et al., *Total knee arthroplasty kinematics. Computer simulation and intraoperative evaluation.* J Arthroplasty, 1998. **13**(2): p. 145-55.
52. Godest, A.C., et al., *Simulation of a knee joint replacement during a gait cycle using explicit finite element analysis.* J Biomech, 2002. **35**(2): p. 267-75.
53. Godest, A.C., et al., *A computational model for the prediction of total knee replacement kinematics in the sagittal plane.* J Biomech, 2000. **33**(4): p. 435-42.
54. Halloran, J.P., S.K. Easley, J. Penmetsa, P.J. Laz, A.J. Petrella, P.J. Rullkoetter, *Effeicient Dynamic Finite Element Rigid Body Analysis of TJR*, in *Summer Bioengineering Conference*2003: Sonesta Beach Resort, Key Biscayne, Florida. p. 551-2.
55. Guess, T.M. and L.P. Maletsky, *Computational modeling of a dynamic knee simulator for reproduction of knee loading.* J Biomech Eng, 2005. **127**(7): p. 1216-21.
56. Siston, R.A., et al., *Coronal plane stability before and after total knee arthroplasty.* Clin Orthop Relat Res, 2007. **463**: p. 43-9.
57. Bertozzi, L., et al., *Knee model sensitivity to cruciate ligaments parameters: a stability simulation study for a living subject.* J Biomech, 2007. **40 Suppl 1**: p. S38-44.
58. Donahue, T.L., et al., *A finite element model of the human knee joint for the study of tibio-femoral contact.* J Biomech Eng, 2002. **124**(3): p. 273-80.
59. Andriacchi, T.P., et al., *Model studies of the stiffness characteristics of the human knee joint.* J Biomech, 1983. **16**(1): p. 23-9.
60. Shi, J.F., et al., *A dynamic model of simulating stress distribution in the distal femur after total knee replacement.* Proc Inst Mech Eng H, 2007. **221**(8): p. 903-12.
61. Weiss, J.A. and J.C. Gardiner, *Computational modeling of ligament mechanics.* Crit Rev Biomed Eng, 2001. **29**(3): p. 303-71.
62. Guess, T.M. and L.P. Maletsky, *Computational modelling of a total knee prosthetic loaded in a dynamic knee simulator.* Med Eng Phys, 2005. **27**(5): p. 357-67.
63. Siston, R.A., et al., *Evaluation of methods that locate the center of the ankle for computer-assisted total knee arthroplasty.* Clin Orthop Relat Res, 2005. **439**: p. 129-35.
64. Siston, R.A., et al., *Intraoperative passive kinematics of osteoarthritic knees before and after total knee arthroplasty.* J Orthop Res, 2006. **24**(8): p. 1607-14.
65. Siston, R.A., et al., *Surgical navigation for total knee arthroplasty: a perspective.* J Biomech, 2007. **40**(4): p. 728-35.

66. Picard, F.D.I.A., Moody, J., Jaramaz, B., inventors, *Probe and associated system and method for facilitating planar osteotomy during arthroplasty.* United States, 2003.
67. Siston, R.e.a., *Intraoperative Passive Knee Kinematics of Osteoarthritic Knees before and after Total Knee Arthroplasty.* The Jornal of Orthopaedic Research, 2006a: p. 1607-1614.
68. Grood, E.S. and W.J. Suntay, *A joint coordinate system for the clinical description of three-dimensional motions: application to the knee.* J Biomech Eng, 1983. **105**(2): p. 136-44.
69. Piazza, S.J., *Muscle-driven forward dynamic simulations for the study of normal and pathological gait.* J Neuroeng Rehabil, 2006. **3**: p. 5.
70. Landon RL, M.H., SJ Piazza, *Robust contact modeling using trimmed NURBS surfaces for dynamic simulations of articular contact.* Comp Methods Appl Mech Eng, 2009. **198**: p. 2339-46.
71. Delp, S.L., et al., *An interactive graphics-based model of the lower extremity to study orthopaedic surgical procedures.* IEEE Trans Biomed Eng, 1990. **37**(8): p. 757-67.